Check for updates

Geochemistry, Geophysics, Geosystems®

AGU ADVANCING EARTH AND SPACE SCIENCES

RESEARCH ARTICLE
10.1029/2024GC012092

Special Collection:
A fresh look at the Caribbean plate geosystems

Seismotectonics and Crustal Structure in the Southern Dominican Republic Offshore Margin: Implications on the Tsunami Potential

J. L. Granja-Bruña[1], J. M. Gorosabel-Araus[1,2], U. ten Brink[3], A. Muñoz-Martín[1,4], A. Rodríguez-Zurrunero[1], S. Leroy[5], A. López-Venegas[6], M. Llorente-Isidro[7], J. Macías Sánchez[8], C. Sánchez-Linares[8], and A. Carbó-Gorosabel[1†]

[1]Applied Tectonophysics Group, Departamento de Geodinámica, Estratigrafía y Paleontología, Universidad Complutense of Madrid, Madrid, Spain, [2]Department of Earth and Atmospheric Sciences, University of Houston, Houston, TX, USA, [3]U.S. Geological Survey, Woods Hole, Ma, USA, [4]Instituto de Geociencias, CSIC-UCM, Madrid, Spain, [5]Sorbonne Université, CNRS, ISTeP, Institut des Sciences de la Terre de Paris, Gières, France, [6]Departamento de Geología, University of Puerto Rico, Mayagüez, Puerto Rico, [7]Area of Geological Hazards and Risks, Geological Survey of Spain (IGME-CSIC), Madrid, Spain, [8]Departamento de A.M., E. e I.O. y Matemática Aplicada, Universidad de Málaga, Málaga, Spain

Abstract Many coastal areas of the southern Dominican Republic experience considerable population pressure accompanied by important economic activity. The southern offshore margin is characterized by significant seismicity and active geological processes. Because of the proximity of the seismogenic and tsunamigenic areas to the coastal regions, large seismic events are likely to result in significant damage. The interpretation of seismotectonic, structural, and morphological data allowed us to characterize the tsunamigenic features. The major tectonic sources involve large shallow faults that are capable of producing earthquakes with magnitudes ranging from Mw7.0 to Mw8.1. These seismic sources could release enough energy to deform and occasionally rupture the seafloor: Muertos frontal thrust, Muertos mega-splay and the Muertos Trough fault zone. In addition, these tectonic sources show significant vertical seafloor deformation with the potential to generate tsunamis. The steeper seafloor slopes show frequent active gravitational processes, but generally have a relatively small size and their tsunamigenic potential is therefore low. However, the Complutense slump is an exception showing ≈30 km3 of mobilized material located along a large active fault. If a similar volume is rapidly mobilized in a single slope failure, it could generate a significant tsunami. The southern coast of the Dominican Republic faces a clear risk due to its proximity to potential tsunamigenic sources (30–50 km), resulting in a very short lead-time for warning. The results of this study provide basic information for future tsunami simulations that ultimately allow practical implementation of tsunami preparedness and protection, and for coastal planning and marine resource use.

Plain Language Summary Many coastal areas in the southern Dominican Republic are densely populated and have significant economic activity. The nearby offshore zone is geologically active, and prone to large earthquakes that can cause severe damage, including associated tsunamis. By studying the region with seismological and geophysical marine data, we identified the main sources of tsunamis related to geological faults. These faults can produce powerful earthquakes (magnitude 7.0–8.1) yielding vertical seafloor movements capable of triggering tsunamis. Steep seafloor slopes in the region often experience landslides due to instability, but most of these landslides are too small to cause tsunamis. However, there are also local massive landslide areas that could trigger a major tsunami. Because these tsunami sources are only 30–50 km from the coast, there would be a little time for warnings. This study provides crucial data to support future tsunami simulations and improve preparedness, coastal planning, and marine resource management in the region.

Key Points:

- Active megathrust structures can generate Mw 7.5–8.1 earthquakes with significant tsunamigenic potential
- The steep seafloor and large earthquakes are prone to submarine landslides triggering tsunamis
- The proximity of seismic and tsunami sources poses an obvious risk of the southern Dominican Republic

†Deceased.

Supporting Information:

Supporting Information may be found in the online version of this article.

Correspondence to:

J. L. Granja-Bruña,
jlgranja@ucm.es

Citation:

Granja-Bruña, J. L., Gorosabel-Araus, J. M., ten Brink, U., Muñoz-Martín, A., Rodríguez-Zurrunero, A., Leroy, S., et al. (2025). Seismotectonics and crustal structure in the southern Dominican Republic offshore margin: Implications on the tsunami potential. *Geochemistry, Geophysics, Geosystems*, *26*, e2024GC012092. https://doi.org/10.1029/2024GC012092

Received 10 DEC 2024
Accepted 7 MAY 2025

Author Contributions:

Conceptualization: J. L. Granja-Bruña, A. Carbó-Gorosabel
Data curation: J. L. Granja-Bruña, A. Carbó-Gorosabel
Formal analysis: J. L. Granja-Bruña
Funding acquisition: A. Carbó-Gorosabel

© 2025 The Author(s). Geochemistry, Geophysics, Geosystems published by Wiley Periodicals LLC on behalf of American Geophysical Union.
This is an open access article under the terms of the Creative Commons Attribution License, which permits use, distribution and reproduction in any medium, provided the original work is properly cited.

1. Introduction

Large earthquakes are common in some retroarc zones and are often larger than those occurring in the forearc area directly nucleated in the subduction plate interface (e.g., Costa Rica in 1991; Suárez et al., 1995; Flores in 1992; Beckers & Lay, 1995; Vanuatu in 1999, Lagabrielle et al., 2003). In addition, if the retroarc region is submerged, it may have a significant tsunamigenic potential (e.g., Flores back-thrust, Chacón-Barrantes & Zamora, 2017; El Limón, 1991; Felix et al., 2022). This is the case of the southern margin of the Dominican Republic, which is the submerged retroarc region of the eastern Greater Antilles Island arc (i.e., Hispaniola and Puerto Rico islands;

15252027, 2025, 6, Downloaded from https://agupubs.onlinelibrary.wiley.com/doi/10.1029/2024GC012092 by Universidad Complutense De, Wiley Online Library on [02/06/2025]. See the Terms and Conditions (https://onlinelibrary.wiley.com/terms-and-conditions) on Wiley Online Library for rules of use; OA articles are governed by the applicable Creative Commons License

Investigation: J. L. Granja-Bruña, J. M. Gorosabel-Araus, U. ten Brink, A. Muñoz-Martín, S. Leroy, A. López-Venegas, M. Llorente-Isidro, J. Macías Sánchez, C. Sánchez-Linares
Methodology: J. L. Granja-Bruña, J. M. Gorosabel-Araus, A. Muñoz-Martín, A. López-Venegas, M. Llorente-Isidro, J. Macías Sánchez, C. Sánchez-Linares, A. Carbó-Gorosabel
Resources: J. L. Granja-Bruña, A. Carbó-Gorosabel
Visualization: J. L. Granja-Bruña, J. M. Gorosabel-Araus, A. Rodríguez-Zurrunero
Writing – original draft: J. L. Granja-Bruña
Writing – review & editing: J. L. Granja-Bruña, J. M. Gorosabel-Araus, U. ten Brink, A. Muñoz-Martín, A. Rodríguez-Zurrunero, S. Leroy, A. López-Venegas, M. Llorente-Isidro, J. Macías Sánchez, C. Sánchez-Linares, A. Carbó-Gorosabel

Figures 1a and 1b). This region is characterized by significant seismic activity and active geological processes (Byrne et al., 1985; Granja-Bruña et al., 2014 and therein references). Because of the proximity of the offshore seismogenic and tsunamigenic areas to the coastal regions, large events are likely to result in significant damage because of earthquakes and tsunamis. The steep seafloor together with large earthquakes and associated submarine mass wasting were successful in triggering tsunamis in the NE Caribbean (Figure 1a, e.g., Engel et al., 2016; Grindlay et al., 2005; Harbitz et al., 2012; López-Venegas et al., 2008, 2014, 2015; NCEI-NOAA database; O'Loughlin & Lander, 2003; Von Hillebrandt-Andrade, 2013).

Many coastal areas of the Dominican Republic undergo considerable population pressure that it is accompanied by important economic activity including tourism, industry, commercial ports, naval bases, and energy facilities, among others. The southern coast is a densely populated region with several important cities such as Santo Domingo, its capital with 3 million of citizens (SD in Figure 1a). According to historical and instrumental records, the southern Dominican Republic has been hit by several major earthquakes as the events of 1615, 1665, 1673, 1684, 1691, 1751, 1860, 1984, 2010 and 2021 among others (Figure 1a; IOC Workshop Reports No 276, 2016). Although the number of damage reports for the events of the 17th and 18th centuries is not sufficient for a good location, they appear to have occurred near the south coast of the Dominican Republic (Flores et al., 2012; ten Brink et al., 2011).

Studies published during the last decade have proposed that the Muertos thrust belt (MTB) has the potential to be a major seismic and tsunami source (MTB in Figure 1b, Dunán-Ávila et al., 2025; Engel et al., 2016; Granja-Bruña et al., 2014; Terrier-Sedan & Bertil, 2021; Scardino et al., 2025). The MTB and associated structures are located less than 100 km from the Dominican Republic coast such that the arriving first waves of a potential tsunami will reach the coastal zones in less than 10 min. The limited awareness of most citizens and the lack of risk reduction strategies put the population and economy of coastal areas at substantial risk in case of large earthquakes and tsunamis (IOC Workshop Reports No 276, 2016).

In this study, we used a combined interpretation of the seismotectonics, crustal structure and seafloor morphology based on the integration of seismological data from public databases together with a large compilation of geophysical ship data. This methodology allowed us to carry out a detailed identification and interpretation of the realistic near-field tsunami sources (i.e., coseismic seafloor deformation and submarine slumping). This information covers an essential part in the characterization of the tsunami processes as the study of hydrodynamics, detection, generation, and probability of occurrence (Didenkulova et al., 2021; Geist et al., 2016). The results of this study form the basis for tsunami modeling of the geometry and size of the tsunami sources, and the impact of these potential tsunami sources on the southern coast of the Dominican Republic.

2. Large Earthquakes and Tsunamis Background

There are historical and instrumental records of earthquakes and tsunamis that affected the southern coast of the Dominican Republic. A large event occurred on the 18th of October of 1751 and destroyed the old city of Azua (AZ in Figure 1a). Santo Domingo also suffered severe damage as well as the villages along the south coast (Flores et al., 2012; ten Brink et al., 2011). The scientific literature shows some controversy about the magnitude and epicenter of this event as well as the possible associated tsunami. On the one hand, some authors suggested that this event was caused by large thrusting in the western termination of the MTB with $M \approx 8.0$ (Ali et al., 2008; Byrne et al., 1985; McCann, 2006). Moreover, these authors suggested that this event triggered a tsunami that mainly impacted the old city of Azua Bay (Moreau de Saint Méry, 1796; Scherer, 1912 and therein references). On the other hand, ten Brink et al. (2011) and Bakun et al. (2012) suggest an alternative solution to the MTB associating this event with the eastern termination of the Enriquillo Fault zone (EFZ) and M_I 7.4–7.5 (Figures 1a and 1b). These later authors strongly disagree with the possibility that this earthquake induced the tsunami because there are no contemporary reports of tsunami in Santo Domingo or elsewhere along the southern coast, suggesting that flooding in the Azua Bay area was likely associated with hurricanes that occurred in October of 1751. Moreover, the old city of Azua is located 6 km inland from the coast at an elevation of 23 m (Bakun et al., 2012). Rodríguez (2019) from fieldwork in the Azua area, suggested that the flooding after the earthquake could be related to widespread soil liquefaction during the strong shaking, and the flooding was not related to tsunamis. The most recent large earthquakes strongly affecting the south coast of the Dominican Republic were the events M7.0 on 12 January 2010, and M7.2 t of 14 August 2021, with the epicentral area along the Southern Peninsula of Haiti (SP in Figure 1b; Calais et al., 2010; Raimbault et al., 2023). The 2010 event triggered two

15252027, 2025, 6, Downloaded from https://agupubs.onlinelibrary.wiley.com/doi/10.1029/2024GC012092 by Universidad Complutense De, Wiley Online Library on [02/06/2025]. See the Terms and Conditions (https://onlinelibrary.wiley.com/terms-and-conditions) on Wiley Online Library for rules of use; OA articles are governed by the applicable Creative Commons License

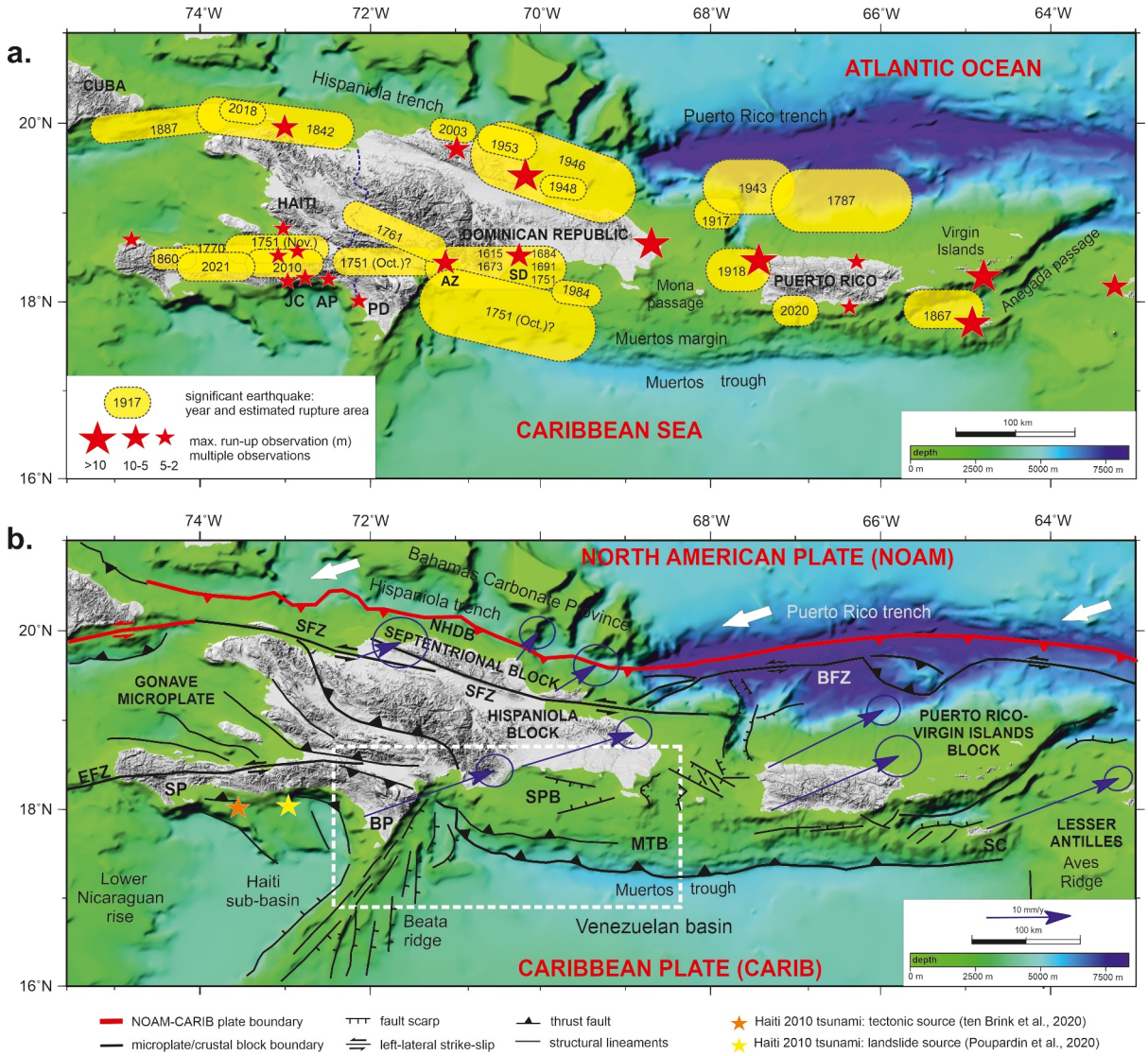

Figure 1. (a) Significant earthquakes and tsunamis in the NE Caribbean (from Ali et al., 2008; Dolan et al., 1998; Engel et al., 2016; Harbitz et al., 2012; López-Venegas et al., 2015; McCann, 2006; O'Loughlin & Lander, 2003; ten Brink et al., 2011; Von Hillebrandt-Andrade, 2013). In the background is a digital elevation model illuminated from the NE (the offshore model is derived from GEBCO data gridded at 1 arc-minute intervals and the onshore digital model comes from SRTM90 mission). JC: Jacmel. AP: Anse-à-Pitres. PD: Pedernales. AZ: Azua. SD: Santo Domingo. (b) Sketched tectonic setting of the NE Caribbean plate. White dashed line inset shows the study area. Background as in (a). Thick white arrows show the relative convergence direction between the North American (NOAM) and Caribbean (CARIB) plates. GPS-derived velocities with respect to the NOAM plate are shown with thin blue arrows, the arrow length being proportional to the displacement rate (modified from Manaker et al., 2008). Error ellipse for each vector represents two-dimensional error, 95% confidence limit. NHDB: North Hispaniola Deformed Belt. MTB: Muertos thrust belt. EFZ: Enriquillo Fault Zone. SFZ: Septentrional Fault Zone. BFZ: Bunce Fault Zone. SC: St. Croix. SPB: San Pedro Basin. SP: Southern Peninsula. BP: Bahoruco Peninsula.

tsunamis (Fritz et al., 2012), one of which hit the south coast of the Southern Peninsula with waves that reached heights of more than 3 m at Jacmel in Haiti (JC in Figure 1a), which is located some 90 km west of Pedernales in the Dominican Republic (PD in Figure 1a). In Pedernales, the 2010 south Haiti tsunami produced 1.3 m run-up, which was observed from the boardwalk (Malecón) and recorded on mobile phone videos by local fishermen. It is noted that only 2 km west of the Pedernales tsunami run-up already exceeded 2 m in Anse-à-Pitre, Haiti (AP in Figure 1a). One of these tsunamis was also recorded on a Caribbean Deep-Ocean Assessment and Reporting of Tsunami buoy (DART 42407) located in the eastern Caribbean Sea and a tide gauge in Santo Domingo. By earthquake finite-fault modeling inversions of the DART waveform, ten Brink et al. (2020) suggested that two dynamically triggered aftershocks with M 6.8 and M 6.5 located on a possibly tectonically active submarine ridge southwest of Southern Peninsula of Haiti may have excited the tsunamis affecting the south coast (Orange star in

15252027, 2025, 6, Downloaded from https://agupubs.onlinelibrary.wiley.com/doi/10.1029/2024GC012092 by Universidad Complutense De, Wiley Online Library on [02/06/2025]. See the Terms and Conditions (https://onlinelibrary.wiley.com/terms-and-conditions) on Wiley Online Library for rules of use; OA articles are governed by the applicable Creative Commons License

Figure 1b). However, Poupardin et al. (2020) suggested an alternative source, most likely a submarine landslide (Yellow star in Figure 1b). They identified a landslide scar 30 km from the epicenter off the southern coast of Haiti at a depth of 3,500 m, where ground acceleration yielded by the earthquake would have been sufficient to trigger slope failure in soft sediments.

3. Tectonic Setting

Along the roughly WNW–ESE- to E–W-trending Hispaniola and Puerto Rico trenches, the North American (NOAM) plate moves with respect to the Caribbean (CARIB) plate at a rate of 20.0 ± 0.4 mm/yr. along an azimuth of 254 ± 1° (DeMets et al., 2010; Figure 1b). A transition from subduction to underthrusting and collision occurs from the Puerto Rico to the Hispaniola trenches. Oblique plate convergence causes strain partitioning (e.g., Calais et al., 2002; Mann et al., 2002), along-strike plate boundary segmentation (e.g., Calais et al., 2016; Oliveira de Sá et al., 2025; Rodríguez-Zurrunero et al., 2020) and crustal block tectonics in the island arc (e.g., Mann et al., 1995; Jansma & Mattioli, 2005; ten Brink & López-Venegas et al., 2012). The highly oblique convergence is mostly accommodated in contractional deformed belts (Northern Hispaniola and Muertos deformed belts; NHDB and MTB, respectively, in Figure 1b) in left-lateral transcurrent systems (Septentrional, Enriquillo, and Bunce fault zones; SFZ, EFZ and BFZ, respectively, in Figure 1b) and diffuse deformation in the Mona and Anegada passages (Figures 1a and 1b).

The eastward motion of Hispaniola has been impeded relative to the interior motion of the CARIB plate since the Eocene due to the oblique collision with the Bahamas Carbonate Province (Calais et al., 2016; Dolan et al., 1998; Mann et al., 2002; Rodríguez-Zurrunero et al., 2018). The collisional stresses in north Hispaniola (i.e., forearc) have been transferred southward because of a highly coupled plate interface, forming a contractional margin along the southern insular slope of Hispaniola (i.e., retroarc; ten Brink et al., 2009; Figure 1b). In the retroarc zone, the deformation style changes along the strike are mostly related to the north-eastward impingement of the aseismic Beata ridge into central Hispaniola (Figure 1b). The impingement from the Upper Miocene onward has caused an along-strike segmentation in the retroarc zone (Granja-Bruña et al., 2014). From east to west, (a) low-angle southward-thrusting along the MTB, (b) collision and uplifting in the Bahoruco peninsula (BP in Figure 1b), and (c) transpression and uplifting in the Southern Peninsula of Haiti (SP in Figure 1b).

The southern Dominican Republic offshore margin shows three main structural and morphological features (Granja-Bruña et al., 2014): The Beata ridge, the Venezuelan basin, and the Muertos margin. The Beata ridge consists of an NE–SW trending, uplifted, and thickened crustal block of the Caribbean Large Igneous Province (CARIB LIP, e.g., Mauffret et al., 2001; Driscoll & Diebold, 1999). The northern Venezuelan basin is bounded by the E–W-trending Muertos trough, with a maximum water depth of 5,500 m. This trough marks the boundary between the interior of the CARIB plate formed by the thickened oceanic crust of the CARIB LIP and the island arc crust (Figure 1b). The CARIB LIP is covered by Upper Cretaceous to recent times sedimentary beds of the large Venezuelan basin. The Muertos margin shows two main features: the Muertos thrust belt and the San Pedro basin (MTB and SPB, respectively, in Figure 1b). The MTB is mainly formed by the offscraping and accretion of pelagic sediments of the Venezuelan basin and turbiditic sediments derived from the island arc (Granja-Bruña et al., 2009). The MTB exhibits a southward transport direction, and it is observable along strike for 650 km from the south of St. Croix in the east (SC in Figure 1b) to the central Hispaniola in the west (Figure 1b; Granja-Bruña et al., 2014, 2015). Slip rates of the current convergence in the western MTB based on regional GPS-derived block models are estimated to be between 4 and 7 mm/yr. of N-S shortening, decreasing eastward to 0.2 mm/yr. south of Puerto Rico (Calais et al., 2016). The SPB consists of a slope basin developed over the rear zone of MTB that accumulates at least 3 km of sediments (Gorosabel-Araus et al., 2021).

4. Data and Methods

Earthquakes are the most frequent source for tsunamis, both as co-seismic seafloor deformation and/or rupture, and as triggering mechanisms of large submarine landslides. To analyze the earthquake occurrence and dominant rupture mechanisms in southeastern Hispaniola, we have used the seismicity data from the National Earthquake Information Center (NEIC-USGS) and the focal mechanisms from the Centroid Moment Tensor Catalog (CMT, Ekström et al., 2012) accessed in March of 2023 (Figure 2; Figure S1 in Supporting Information S1). Focal mechanisms are a valuable resource to characterize the source of earthquake-induced tsunamis because of the connection between the tsunami generation and the type of faulting (e.g., Iida, 1970). The shallow and large

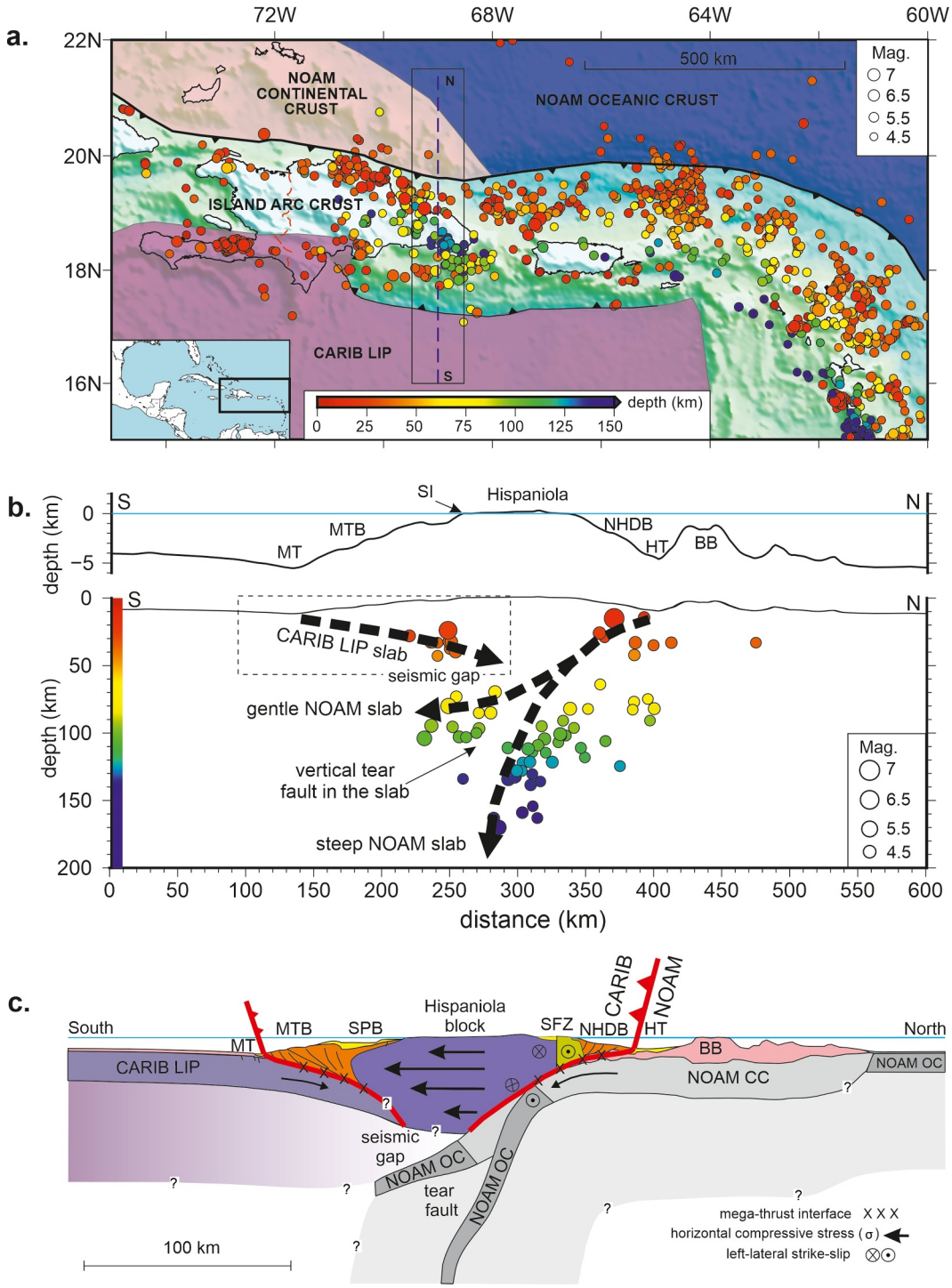

Figure 2. Regional seismicity and conceptual model. NOAM OC: North American oceanic crust. NOAM CC: North American continental crust. CARIB LIP: Caribbean Large Igneous Province. BB: Bahamas Banks. HT: Hispaniola Trench. NHDB: North Hispaniola Deformed Belt. SFZ: Septentrional Fault Zone. SPB: San Pedro Basin. MTB: Muertos Thrust belt. MT: Muertos Trough. SI: Saona island. (a) Seismicity map of the NE Caribbean plate boundary zone. Earthquake data come from the NEIC-USGS filtered by magnitudes above 4.5. See legend for interpretation. The rectangular area represents the compartment that includes the hypocenters plotted in (b). The dashed line shows the location of sections of (b, c). (b) Top: Topo-bathymetric profile across the island arc exaggerated vertically by 15 times. Bottom: Cross-section of seismicity. See location in (a) and plotted hypocenter data including events located to ≈50 km each side. The inferred geometry of the top of the downgoing NOAM and CARIB LIP slabs is indicated by heavy dashed lines. The dashed inset shows the location of Figure 4b. (c) Conceptual tectonic cross-section across the NOAM-CARIB plate boundary in eastern Hispaniola (modified from Rodríguez-Zurrunero et al., 2020; ten Brink et al., 2009). See location in (a).

15252027, 2025, 6, Downloaded from https://agupubs.onlinelibrary.wiley.com/doi/10.1029/2024GC012092 by Universidad Complutense De, Wiley Online Library on [02/06/2025]. See the Terms and Conditions (https://onlinelibrary.wiley.com/terms-and-conditions) on Wiley Online Library for rules of use; OA articles are governed by the applicable Creative Commons License

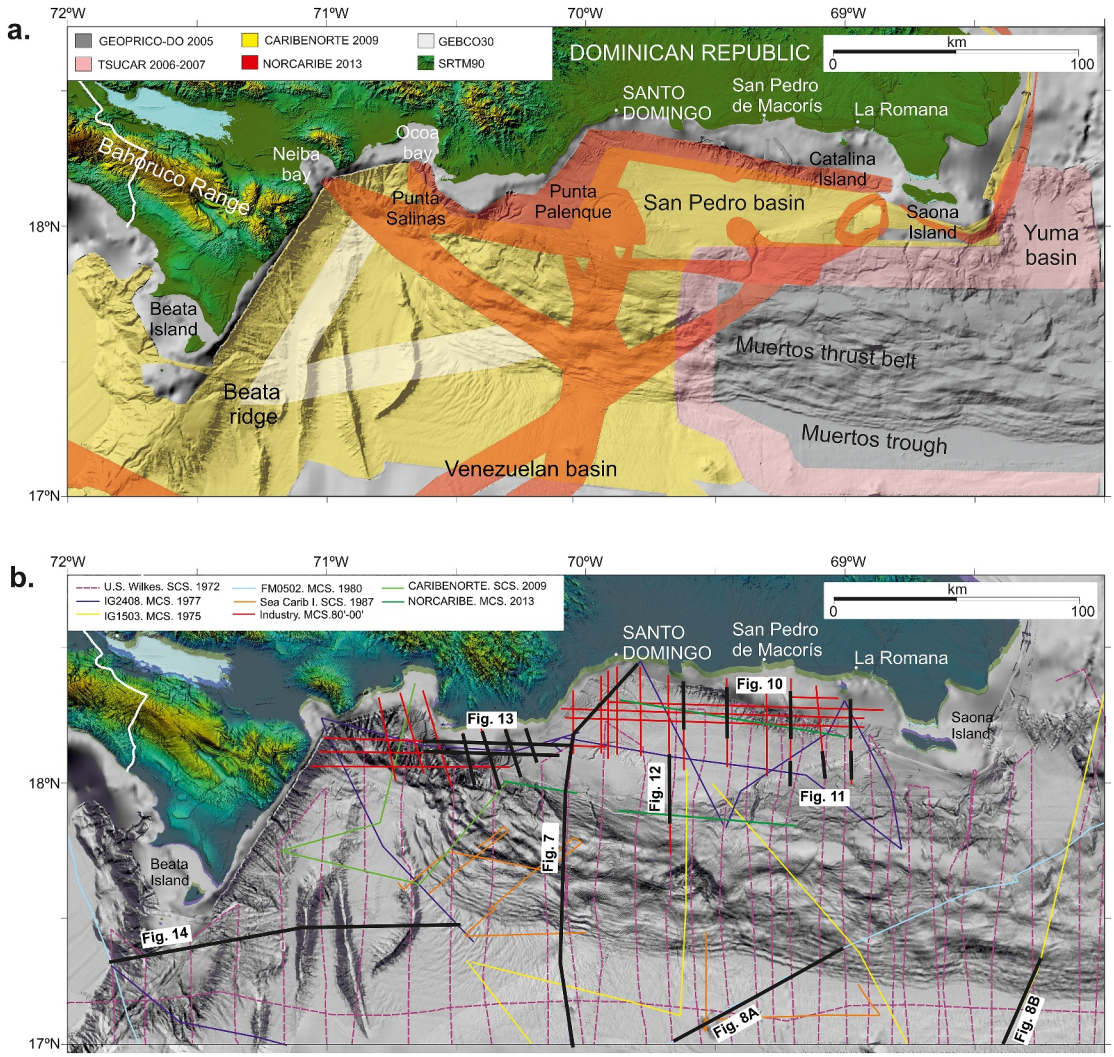

Figure 3. Ship data set (See also Tables S1 and S2 in Supporting Information S2). (a) Multibeam cruises are coded by color. DEM derived from a compilation of multibeam bathymetry data (200 m of resolution) and completed offshore with data from GEBCO (30 s of resolution) and onshore with data from SRTM90 (90 m of resolution) public data sets (Farr et al., 2007; Weatherall et al., 2015). (b) 2D seismic reflection data set used in this study. DEM as in (a). Seismic cruises are coded in color. MCS: Multi-channel Seismic. SCS: Single-channel Seismic. Thick black lines show the seismic sections presented in this manuscript.

earthquakes in offshore areas are the more realistic tsunami sources because they yield strong shaking, deformation and/or rupture of the seafloor. Therefore, we start our study by reviewing and analyzing the spatial distribution and type of the $M > 4.5$ seismicity in the NE Caribbean. We use the conceptual tectonic plate models to exclude deeper events related to subducted slabs and with no significant tsunamigenic potential (e.g., Okal, 2017). Then, we focus on the south-eastern Hispaniola analyzing the shallow seismicity and focal mechanisms (depth <50 km) to identify seismic sources with potential to deform/rupture the seafloor and trigger submarine landslides.

In active tectonic settings, the seafloor morphology can be interpreted in terms of the surface expression of the active underlying crustal structure and associated sedimentary processes. The combined study of bathymetry and seismic data is a key to understand active deformational, sedimentary and landslide processes. From 2005, most of the southern insular slope of the Dominican Republic was mapped with high-resolution swath bathymetry (Figure 3a). Several deep-ocean cruises led by Spanish and USA institutions were coordinated to get a full seafloor coverage (Table S1 in Supporting Information S2, Andrews et al., 2014; Granja- Bruña et al., 2014). For this study, the data sets were homogenized and merged on a surface with a regular grid interval of 200 m. Where there was no multibeam bathymetry coverage, the grid was complemented by the GEBCO Digital Atlas

15252027, 2025, 6, Downloaded from https://agupubs.onlinelibrary.wiley.com/doi/10.1029/2024GC012092 by Universidad Complutense De, Wiley Online Library on [02/06/2025]. See the Terms and Conditions (https://onlinelibrary.wiley.com/terms-and-conditions) on Wiley Online Library for rules of use; OA articles are governed by the applicable Creative Commons License

15252027, 2025, 6, Downloaded from https://agupubs.onlinelibrary.wiley.com/doi/10.1029/2024GC012092 by Universidad Complutense De, Wiley Online Library on [02/06/2025]. See the Terms and Conditions (https://onlinelibrary.wiley.com/terms-and-conditions) on Wiley Online Library for rules of use; OA articles are governed by the applicable Creative Commons License

with a 30-arc-second resolution (Weatherall et al., 2015). The study area has an extended coverage of 2D single-channel and multi-channel seismic data (Figure 3b, Table S2 in Supporting Information S2). The data quality is variable because the seismic data set includes profiles acquired between 1971 and 2013 with different instruments and systems. Legacy post-stack MCS data, when possible, were reprocessed to obtain the cleanest/balanced seismic images to aid interpretation. The processing workflow using Globe Claritas (Academic license under Universidad Complutense de Madrid) includes spectral whitening, coherency enhancement, and standard post-stack f–k migration. The combined interpretation of seismic and swath bathymetry data allowed us to interpret with reasonable confidence the large structures deforming the seafloor.

From the integration of seismotectonic, structural, and morphological data, we carried out the identification and characterization of the tsunamigenic tectonic and landslide features. This characterization provides constraints on the spatial location, size, geometry, and rupture mechanism of the tectonic sources that allows at the same time to obtain the magnitude of potential maximum seismic events estimated using semi-empirical relationships (Wells & Coppersmith, 1994).

5. Data Analysis and Interpretation

5.1. Regional Seismicity and Subducted Slabs Geometry

In the NE Caribbean, earthquakes with magnitudes above 4.5 are mostly nucleated along the subduction-collision zone between the NOAM and CARIB plates (Figures 1 and 2a). Also, many events are associated with large intra-arc faults such as the EFZ and SFZ and in areas of more diffuse deformation such as the Mona and Anegada passages. The overall seismicity occurs along an E–W trending band of 200 km width constrained between the compressive deformation fronts flanking the island arc (Figure 2a), the N-verging NHDB and the Puerto Rico accretionary prism in the forearc and the S-verging MTB in the retroarc (Figure 1b). Along the Lesser Antilles subduction zone, the spatial distribution of earthquakes deeper than 50 km can be reasonably ascribed to the W-dipping NOAM slab (Figure 2a, e.g., Dolan et al., 1998). However, the seismicity pattern becomes very diffuse in the Puerto Rico trench, the Mona passage and the eastern Hispaniola region (Figure 2). Eastern Hispaniola is where the transition from oblique subduction of the NOAM oceanic crust (NOAM OC) roughly takes place along the Puerto Rico trench to oblique underthrusting and collision of a thicker crust of the NOAM continental crust (NOAM CC; Bahamas Carbonate Province) along the Hispaniola trench (Rodríguez-Zurrunero et al., 2020). That diffuse spatial pattern of seismicity makes the definition of the downward slab geometries in eastern Hispaniola difficult. Several geodynamic scenarios have been suggested. Ludwig (1989), Dillon et al. (1996), and Dolan et al. (1998) proposed opposite dipping slabs colliding in the upper mantle: a gentle N-dipping CARIB LIP slab pushing down on a steep S-dipping NOAM slab. Double subduction models differ in the continuity S-dipping NOAM slab: a continuous slab (Dolan et al., 1998; McCann & Sykes, 1984) and a detached slab (Dillon et al., 1996; García-Senz et al., 2017). The existence of an N-dipping CARIB LIP slab subducting beneath eastern Hispaniola was proposed based on a diffuse, shallow and gentle N-dipping zone of seismicity (Byrne et al., 1985). Over the last decades, studies based on observations of the deformational features along the MTB (Granja-Bruña et al., 2009, 2014, 2015) combined with analog and geophysical modeling (Granja-Bruña et al., 2010; Llanes et al., 2012; ten Brink et al., 2009) have questioned the existence of a subducting N-verging CARIB LIP slab sinking into the upper mantle. These studies suggest that a CARIB LIP slab underthrusts the southern Hispaniola Island margin but does not penetrate the upper mantle. This situation implies the absence of a slab pull driving mechanism (cf., Stern & Gerya, 2018), that is, the lack of a true subduction of the CARIB LIP. In addition, studies based on large-scale seismic tomography (ten Brink et al., 2013; van Benthem et al., 2014; Xu et al., 2015) and receiver functions (Kumar et al., 2023) are successful in imaging an S-dipping NOAM slab, but not conclusive related to the existence of an N-dipping CARIB LIP slab. Tomography results image a local shallow zone of high velocity in the southern margin that is interpreted *sensu lato* as the CARIB LIP slab. Recent studies from the harmonic decomposition of receiver functions documented an anisotropic layer at ≈22 km of depth beneath the Saona Island (Figure S2b in Supporting Information S1), which may correspond to the underthrusting CARIB LIP slab (Kumar et al., 2023). These latter authors also note that if there were a CARIB LIP subducted slab, its velocity anomaly would be expected over a broader area along the Muertos margin, but it was not identified.

The representative cross-section of seismicity in eastern Hispaniola shows two clusters of events shallower than 40 km that can be ascribed to the compression and shortening on both sides of the island arc along the NHBD and MTB (Figure 2b). The NHDB is accommodating the NE–SW-trending oblique convergence between the NOAM

15252027, 2025, 6, Downloaded from https://agupubs.onlinelibrary.wiley.com/doi/10.1029/2024GC012092 by Universidad Complutense De, Wiley Online Library on [02/06/2025]. See the Terms and Conditions (https://onlinelibrary.wiley.com/terms-and-conditions) on Wiley Online Library for rules of use; OA articles are governed by the applicable Creative Commons License

and CARIB plates, while the MTB accommodates the N─S-trending orthogonal convergence between the CARIB LIP and the island arc. The shallow events beneath the NHDB can be related to the upper zone of an S-dipping NOAM slab that continues up to 160 km of depth. At the same time, this deep S-dipping zone of seismicity could be separated/fragmented into two sub-zones: a deeper and steeper sub-zone (70–180 km of depth) representing the subducted NOAM slab (likely Atlantic oceanic crust beneath the Mona passage) and an intermediate and gentler sub-zone (70–110 km of depth) beneath the south-eastern Hispaniola also representing the subducted NOAM slab (likely Atlantic continental/transitional crust of the Bahamas Carbonate Province). The significant change in the geometry of both subducting slabs was suggested to be accommodated through a vertical slab tear fault (Rodríguez-Zurrunero et al., 2020). This interpretation is based on the clustering of seismicity and the distinct oceanic or continental nature of the incoming Atlantic subducting crust: the Atlantic oceanic crust is thinner and denser, forming a steeper NOAM oceanic slab (continuous or detached) and the transitional or continental crust is thicker and relatively buoyant forming a gentle NOAM slab.

In the south-eastern Hispaniola region, the zone of seismicity shows maximum depths up to 40 km and is only circumscribed to the retroarc region. Those earthquakes would be ascribed to the deformation driven by a gentle shallow N-dipping CARIB LIP slab underthrusting beneath the island arc (Figures 2b and 2c). Events would be mostly nucleated at the interface between the CARIB LIP slab and the island arc crust. This zone of seismicity is disconnected from the zones ascribed to the NOAM slab through a seismic gap. This seismic gap is coherent with the Moho located ≈30 km of depth beneath central Hispaniola estimated by both active and passive seismic studies (Kumar et al., 2020; Nuñez et al., 2019; Possee et al., 2021). The seismic gap beneath central Hispaniola suggests that the northward underthrusting of the CARIB LIP slab is limited and does not enter the upper mantle (Figure 2c).

In summary, in the eastern Hispaniola and Mona passages, the intermediate seismicity (70–110 km of depth) is related to the deep NOAM slabs, while <40 km of depth seismicity is related to shallow NOAM and CARIB LIP slabs. The CARIB LIP slab underthrusting the island arc is a result of the compression between the interior of the CARIB plate and the island arc and does not represent a true subduction zone. This shallow seismicity zone can be better understood in a model of a retro-wedge forming part of a bi-verging crustal wedge system surrounding the eastern Greater Antilles Island arc during unidirectional subduction along the Hispaniola and Puerto Rico trenches (Figures 2c, Rodríguez-Zurrunero et al., 2020; ten Brink et al., 2009).

5.2. Spatial Analysis of the Local Seismicity and Focal Mechanisms

The occurrence of shallow earthquakes of significant magnitude (i.e., <50 km of depth and $M > 4.5$) in the south-eastern Hispaniola takes place along a WNW─ESE-trending diffuse band of seismicity with a predominance of reverse focal mechanisms (Figures 4a and 5a). These characteristics are coherent with the overall N-S component of shortening between the interior of the CARIB plate and the island arc suggested by GPS-derived velocities and local focal mechanism slip modeling (4–7 mm/yr. of N-S shortening; Calais et al., 2016) and the observations in the structure of the MTB (Granja-Bruña et al., 2014). The 3D analysis of this band of seismicity and the distinctive focal mechanisms allows us to identify two groups of earthquakes (Figures 4 and 5); (a) the Muertos Group, mainly located on the MTB and SPB where the seismicity is distributed in a E─W elongated zone, the hypocenters vary between 10 and 45 km of depth, and the focal mechanisms are mainly reverse with E─W-trending nodal planes (Figures 5b and 5c); and (b) the Beata Indenter Group located onshore in the eastern termination of the Central, Neiba, and Bahoruco ranges where the seismicity is distributed in a NE─SW elongated zone, the hypocenters vary between 10 and 30 km and focal mechanisms coexisting strike-slip, oblique reverse and pure reverse (Figure 5d).

The Muertos and Beata Indenter groups of seismicity are coherent with the along-strike segmentation of the southern margin of Hispaniola (Granja-Bruña et al., 2014). The main cause of the segmentation is the significant change in the along-strike structure and thickness of the incoming CARIB LIP. In the east, the CARIB LIP is formed by the 12–14 km-thick oceanic plateau underlain the Venezuelan basin, and in the west, the CARIB LIP is formed by the thick oceanic crust of the Beata ridge (at least 25 km-thick: Nuñez et al., 2016). This change in the CARIB LIP thickness takes place at a relatively short distance and favored by means of a passive NE─SW-trending sub-vertical tear fault located in the eastern flank of the Beata ridge (Granja-Bruña et al., 2014). Because of the N─S shortening between the island arc and the CARIB LIP, there is differential accommodation along the strike. The shortening is accommodated in the east due to the low-angle

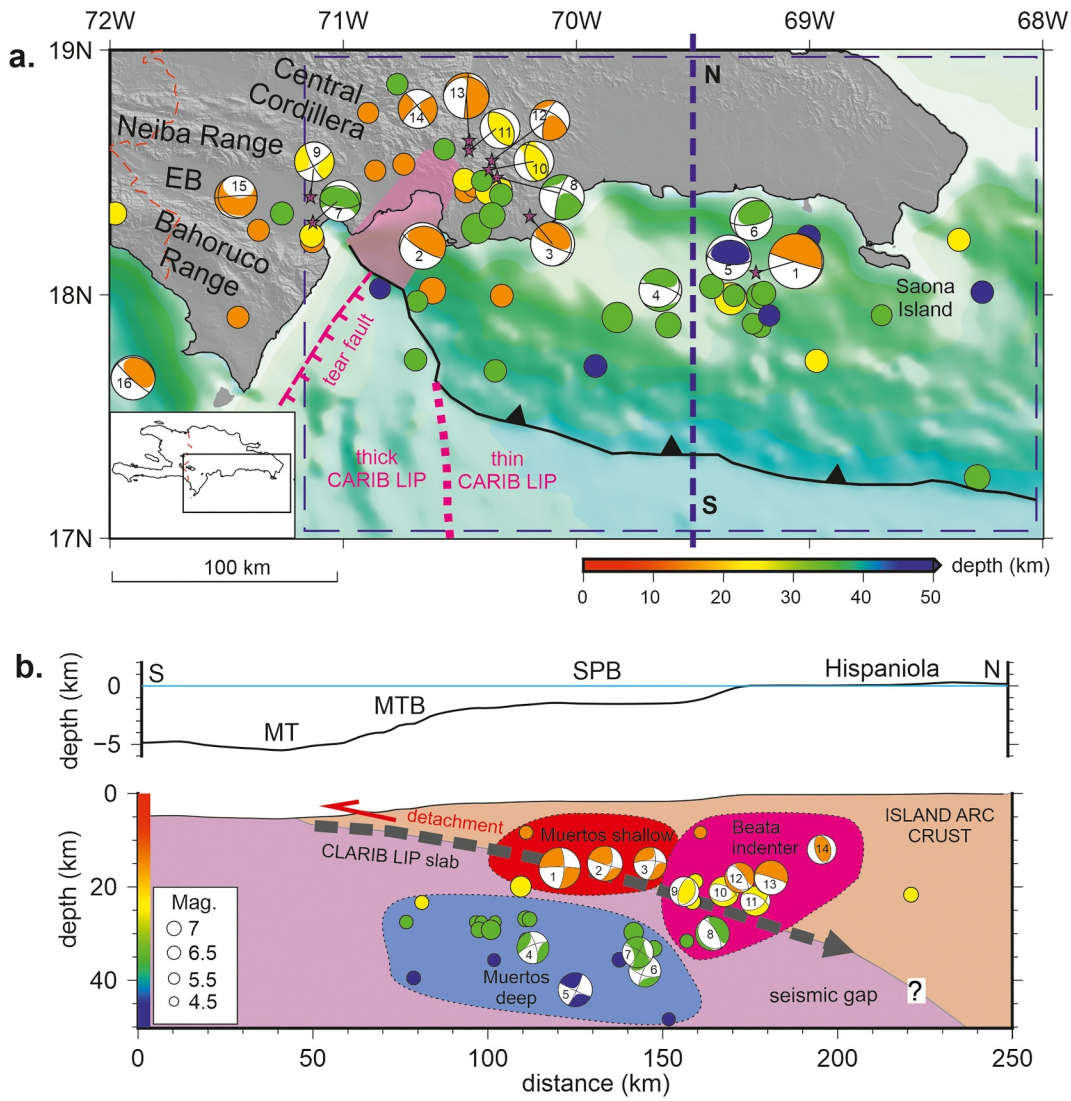

Figure 4. (a) Seismicity map of the south-eastern Hispaniola. Earthquake data as in Figure 2a but focal depths less than 50 km. Focal mechanism solutions come from the Harvard CMT catalog. Hypocenters and focal mechanisms are shown in color code based on depth. The dashed rectangular area represents the compartment that includes the hypocenters plotted in the seismicity cross-section of (b). The purple area shows the estimated extension of the Beata indenter. (b) Top: Topographic profile exaggerated vertically 15 times. See location in (a). SPB: San Pedro Basin. MTB: Muertos Thrust Belt. MT: Muertos Trough. Bottom: Cross section of seismicity plotted in (a). The inferred geometry of the top of the downgoing CARIB LIP slab is indicated by a heavy dashed line.

underthrusting of the Venezuelan basin beneath the island arc and in the west by the impingement of the Beata ridge against the island arc (Granja-Bruña et al., 2014). The significant change in the along-strike crustal thickness is documented by Nuñez et al. (2019) from E–W wide-angle velocity modeling showing an ≈18 km-thick crust in the Venezuelan basin and a ≈30 km-thick crust in the Bahoruco Range (Figure 4a). This segmentation is also in agreement with the hypocenters being deeper (up to 45 km) in the east related with the underthrusting of the CARIB LIP, and shallower (up to 25 km) in the west related with the collision of the CARIB LIP (Figure 4a). This last observation was also documented by Rodríguez et al. (2018) throughout the analysis of seismological data recorded in a local seismic network in the western Bahoruco Range. Their results showed that most of the small magnitude seismicity is located shallower than 25 km of depth in agreement with the along-strike segmentation where shallow seismicity takes place in the collision region while deeper seismicity occurs in the underthrusting region.

15252027, 2025, 6, Downloaded from https://agupubs.onlinelibrary.wiley.com/doi/10.1029/2024GC012092 by Universidad Complutense De, Wiley Online Library on [02/06/2025]. See the Terms and Conditions (https://onlinelibrary.wiley.com/terms-and-conditions) on Wiley Online Library for rules of use; OA articles are governed by the applicable Creative Commons License

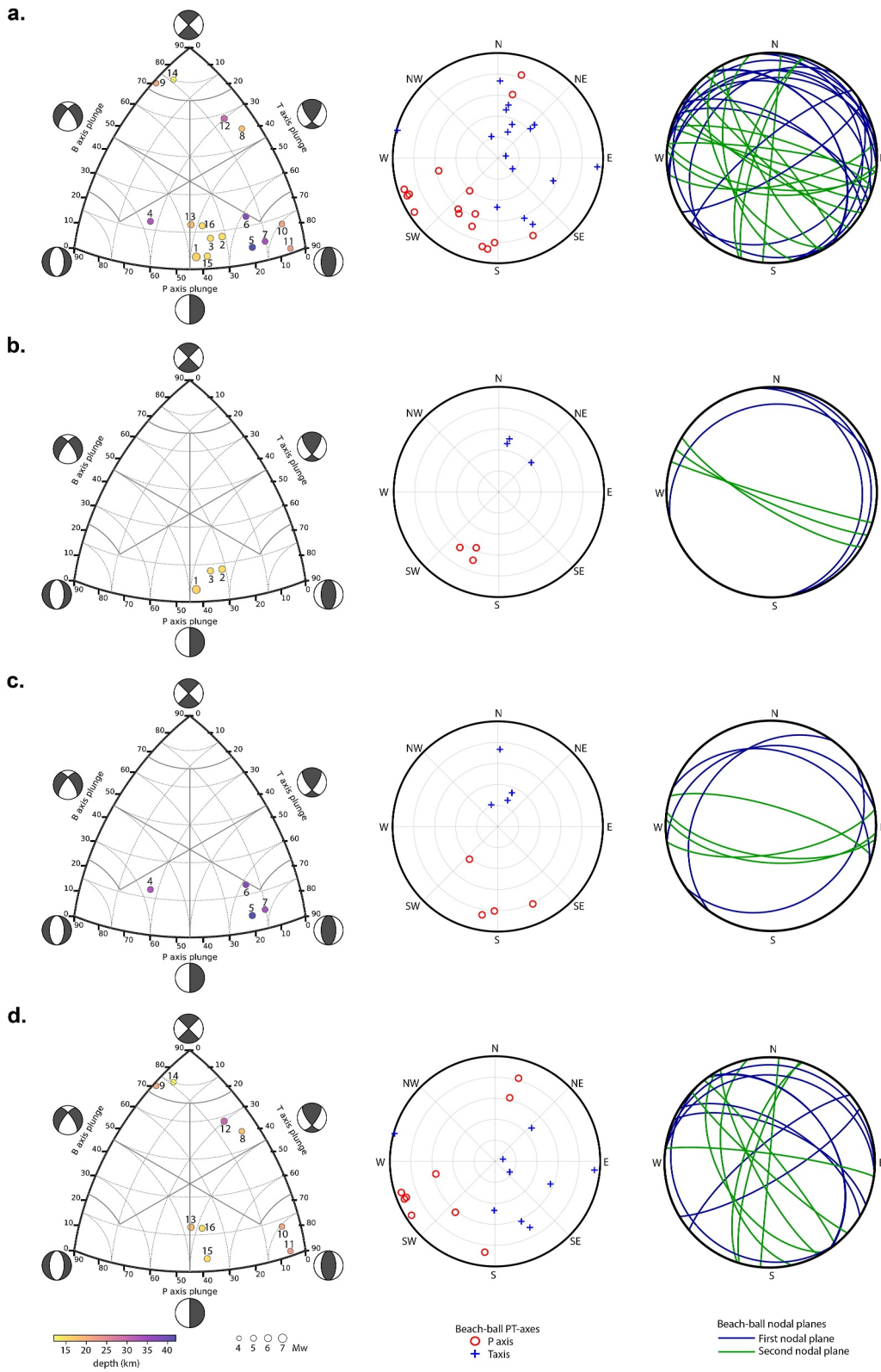

Figure 5. Classification of focal mechanisms of the CMT catalog in the study area (Figures 4a and 4b) in strike-slip, reverse, normal and odd (Frolich, 1992). Plot of the triangle diagram (Álvarez-Gómez, 2019), and PT-axes and nodal planes into the polar diagrams (Hallo et al., 2019). See legend for interpretation. (a) All focal mechanisms in the study area. (b) Muertos Shallow Sub-group. (c) Muertos Deep Sub-group. (d) Beata Indenter Group.

15252027, 2025, 6, Downloaded from https://agupubs.onlinelibrary.wiley.com/doi/10.1029/2024GC012092 by Universidad Complutense De, Wiley Online Library on [02/06/2025]. See the Terms and Conditions (https://onlinelibrary.wiley.com/terms-and-conditions) on Wiley Online Library for rules of use; OA articles are governed by the applicable Creative Commons License

15252027, 2025, 6, Downloaded from https://agupubs.onlinelibrary.wiley.com/doi/10.1029/2024GC012092 by Universidad Complutense De, Wiley Online Library on [02/06/2025]. See the Terms and Conditions (https://onlinelibrary.wiley.com/terms-and-conditions) on Wiley Online Library for rules of use; OA articles are governed by the applicable Creative Commons License

5.2.1. Muertos Group

The focal mechanisms in the Muertos Group show a predominant reverse component, divided into two sub-groups based on the focal depth (Figure 4) and on the dip and orientation of the nodal planes (Figures 5b and 5c):

The Muertos Shallow Sub-group is formed from the three events with focal depths between 20 and 25 km showing a preferential thrust motion with one N-dipping low-angle nodal plane and the other sub-vertical (Events 1, 2, and 3 in Figure 4). These three focal mechanisms can be ascribed to the structure and dynamics of the MTB, where the N-dipping low-angle nodal plane is coherent with the large thrust faults identified in the MTB (Granja-Bruña et al., 2014). Assuming a reasonable uncertainty in the focal mechanism location, these events could be nucleated along the low-angle basal detachment or in any of the numerous large N-dipping reverse faults forming the MTB (See Section 5.3.2). These three events are coherent with recent studies from harmonic decomposition of receiver functions that documented an anisotropic layer at a depth of ≈22 km beneath the Saona Island (Figure 4a), which may correspond to the top of the underthrusting CARIB LIP slab (Kumar et al., 2023). The largest event of this sub-group occurring in 1984 with Ms 6.7 exhibits a near-pure thrust motion along an E–W-trending plane and was used as main evidence to support the subduction along the Muertos trough (Byrne et al., 1985; Event 1 in Figure 4).

The Muertos Deep Sub-group includes four events in an equivalent distance from Muertos Trough to the first sub-group, but with focal depths between 30 and 45 km. They are likely located beneath the basal detachment (Events 4, 5, 6 and 7 in Figure 4). Mechanisms 5, 6, and 7 show near-pure reverse solutions with steep nodal planes and mechanism 4 is oblique with a small normal component (Figures 5b and 5c). These varieties of reverse and normal focal mechanisms with steeply dipping planes are common intra-slab events and are probably associated with flexural slip processes along the incoming slab (e.g., Romeo & Álvarez-Gómez, 2018). Because of their depth, this sub-group could be ascribed to CARIB LIP intra-slab events. This interpretation agrees with gravity modeling that suggests that the CARIB LIP crust beneath the Hispaniola extends at least 60 km northward of the Muertos trough (Granja-Bruña et al., 2010).

The Muertos Shallow Sub-group shows a P axis orientation between 200° and 215° that is compatible with NE-SW shortening (Figure 5b) and the Muertos Deep Sub-group an orientation 155° and 223° that is also compatible with a N-S shortening (Figures 5b and 5c). Therefore, the focal mechanism of the Muertos Group agrees with the overall NE-SW shortening between the CARIB LIP and the island arc (Figure 5a).

5.2.2. Beata Indenter Group

The focal mechanisms in the Beata Indenter Group are located between 10 and 25 km of depth and show variable focal solutions from pure to oblique reverse and strike-slip (Figures 4 and 5d). The orientation of the P axis shows a wide range with a predominant population of events between 185° and 265° suggesting a NE─SW component of shortening (Figure 5d). Pure reverse mechanisms show NW─SE trending nodal planes dipping ≈50-60° (Events 10 and 11 in Figure 4). Oblique reverse mechanisms show NW─SW to NEN─SWS trending nodal planes dipping more than 60°, and with a predominant strike-slip component (Events 8 and 12 in Figures 4 and 5d). Strike-slip mechanisms show NW─SE to NE─SW trending nodal planes (Events 9 and 14 in Figures 4 and 5d). The coexistence of variable focal mechanisms from pure reverse and strike-slip is common in indentation settings where the stress field varies in agreement with the geometry of the indenter (e.g., Reiter et al., 2018). Reverse mechanisms predominate in the front of the indenter and oblique to strike-slip predominate in the sides of the indenter (Estimated location of the indenter in Figure 4a; Escuder-Viruete et al., 2024; Hernaiz-Huerta et al., 2007). The oblique and strike-slip mechanisms 8 and 12 show one nodal plane oriented NE─SW with a right-lateral component that is coherent with ruptures along the eastern corner of the indenter. The pure reverse events 10 and 11 show NW-SE trending nodal planes that are coherent with ruptures in the frontal part of the indenter. The strike-slip event 14 shows a nodal plane-oriented NE-SW with a left-lateral component that is coherent with ruptures along the western corner of the indenter.

Classification of focal mechanisms from the CMT catalog (Frolich, 1992) shows some exceptions to the previous classification with events that show low double couple percentage and are plotted in the odd region of the triangle diagram (Events 13, 15 and 16 in Figures 4 and 5d). These events could be associated with complex ruptures; (a) Event 13 is in the Central Cordillera having an almost pure solution showing a vertical N─S nodal plane and a low angle E─W nodal plane. This event could be interpreted as a rupture in the frontal part of the indenter; (b) Event

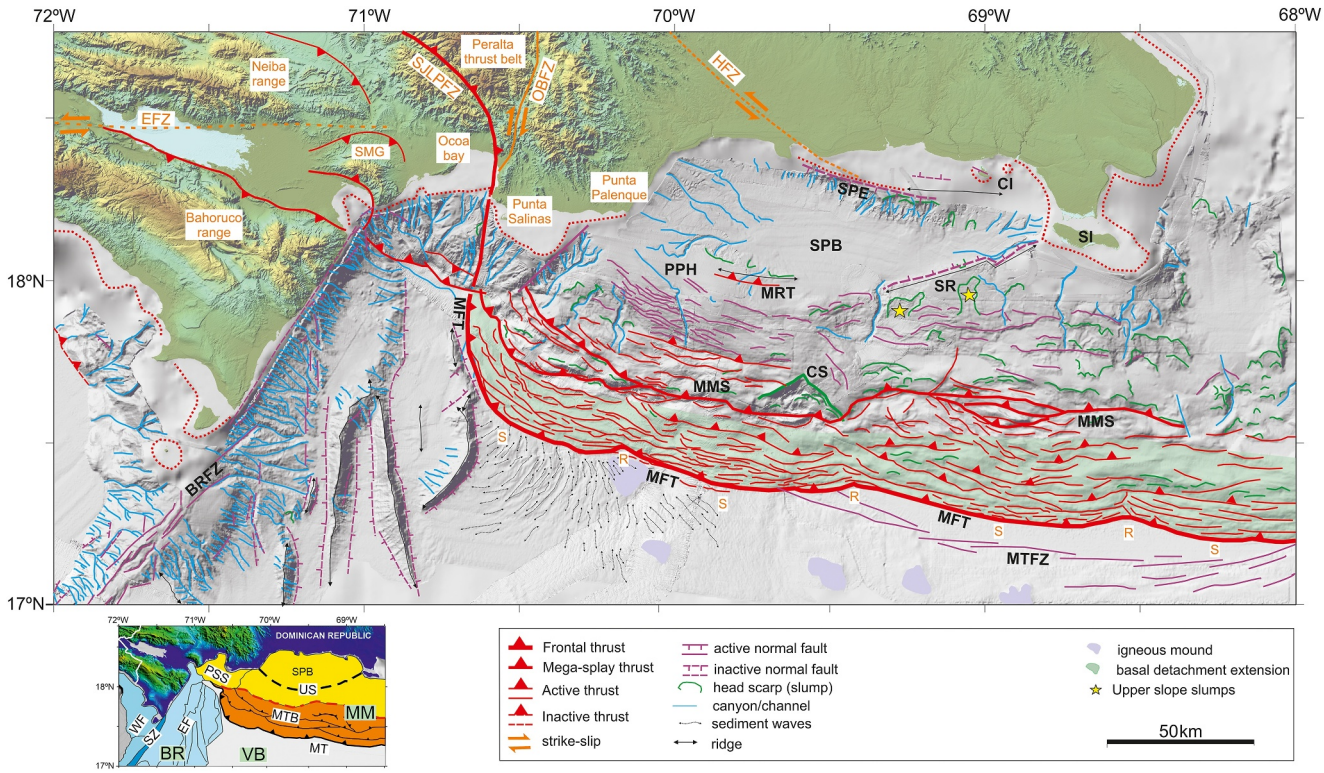

Figure 6. Morphotectonic interpretation (modified from Granja-Bruña et al., 2014). EFZ: Enriquillo fault zone. SJLPFZ: San Juan-Los Pozos fault zone. OBFZ: Ocoa-Bonao fault zone. HFZ: Hispaniola fault zone. SMG: Sierra de Martín García. MFT: Muertos Frontal Thrust. MMS: Muertos Mega-splay. MRT: Muertos Rear Thrust. MTFZ: Muertos Trough Fault Zone. BRFZ: Beata Ridge Fault Zone. CS: Complutense slump. PPH: Punta Palenque High. SPB: San Pedro Basin. SPE: San Pedro Escarpment. SR: Saona Ridge. CI: Catalina Island. SI: Saona Island. R and S: Recess and Salient in the deformation front, respectively. The inset map shows the division into three morphotectonic provinces (VB: Venezuelan basin; BR: Beata ridge; MM: Muertos margin) and different sub-provinces (WF: Western flank of Beata ridge; SZ: Beata summit zone; EF: Eastern flank of Beata ridge; PSS: Punta Salinas slope; MT: Muertos trough; MTB: Muertos thrust belt; US: Upper slope; SPB: San Pedro basin). The thick red dashed line marks the boundary between the MTB and the US. Thick black dashed line marks the structural high formed by the Punta Palenque High in the west and the Saona Ridge in the east.

15 in the Enriquillo basin has vertical E—W and NW—SE sub-horizontal nodal planes. This event could be associated with the large NW-SE thrust faults bounding the Enriquillo basin and/or with the eastern termination of the EFZ (Rodríguez et al., 2018); and (c) Event 16 located offshore in the Haiti sub-basin at the base of the island slope has a sub-horizontal E—W and vertical NW—SE nodal planes and could be related with the active thrusting along the insular margin slope of the Southern Peninsula of Haiti (SP in Figure 1b; ten Brink et al., 2020).

The focal solutions of the Beata Indenter Group agree with structural geological observations in the Ocoa Bay and the eastern termination of the Central Cordillera showing large active faults with NE—SW and WNW—EWE orientations (Escuder-Viruete et al., 2023, 2024; Hernaiz-Huerta et al., 2007). The magnitudes of this group are slightly lower than in the Muertos Shallow Sub-group because of the predominance of diffuse deformation and intense fault segmentation (Figure 6; Calais et al., 2022; Escuder-Viruete et al., 2024). In a recent study based on fieldwork and optically stimulated luminescence geochronology in the south-central Dominican Republic, Escuder-Viruete et al. (2023) suggested that the frontal thrust of MTB can be connected onshore along the eastern Ocoa Bay with a newly proposed fault named the Ocoa-Bonao-La Guacara fault zone (OBFZ in Figure 6). This fault consists of N—S trending and a broad zone of right-lateral strike-slip deformation that can be mapped along 250 km in the interior of the Dominican Republic. The authors suggest that this fault is responsible for the seismicity of the south-central Dominican Republic (i.e., the Beata Indenter Group defined in this study). Right-lateral strike-slip events 8 and 12 are compatible with ruptures along the OBFZ. This new interpretation disagrees with previous studies based on onshore gravity (Ayala et al., 2017) and onshore-offshore gravity and magnetic anomalies (Gorosabel-Araus et al., 2021) that interpreted the Bonao Fault as continuing eastward to the offshore San Pedro basin.

15252027, 2025, 6, Downloaded from https://agupubs.onlinelibrary.wiley.com/doi/10.1029/2024GC012092 by Universidad Complutense De, Wiley Online Library on [02/06/2025]. See the Terms and Conditions (https://onlinelibrary.wiley.com/terms-and-conditions) on Wiley Online Library for rules of use; OA articles are governed by the applicable Creative Commons License

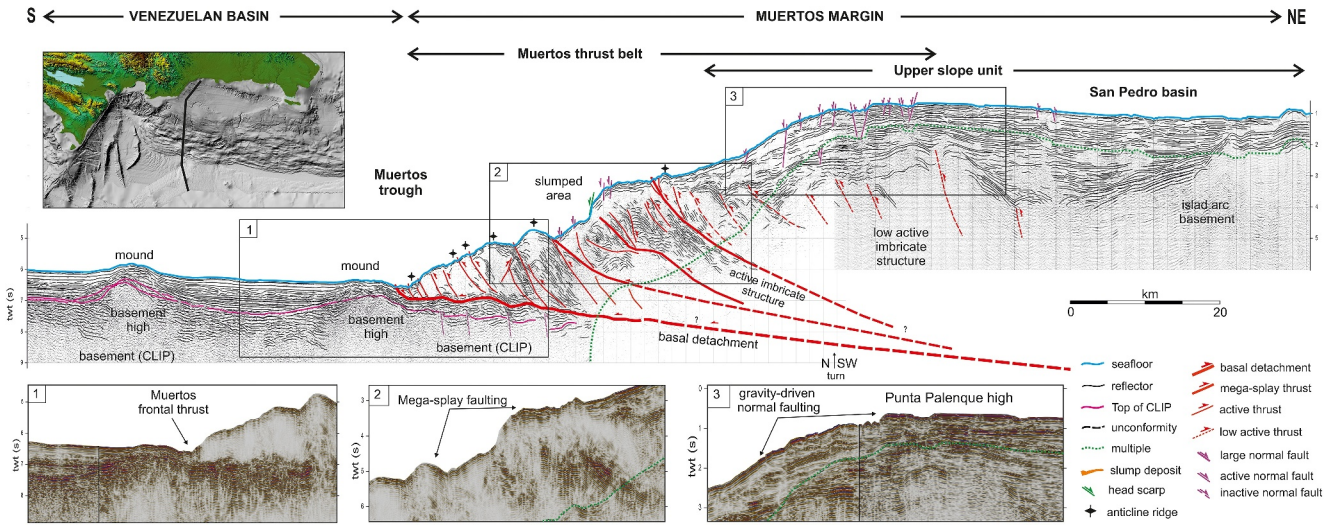

Figure 7. Line drawing interpretation of a regional across-strike seismic section of the Muertos margin (modified from Granja-Bruña et al., 2014). V.E. is 6.6× on the seafloor. See map inset for location and legend for details. Insets show enlarged sectors of: 1) Muertos frontal trust; 2) Mega-splay and associated slumping; and 3) Punta Palenque high.

5.3. Crustal Structure and Seafloor Morphology

This section is dedicated to the identification and geological characterization of both tectonic and landslide sources of potential tsunamis. Granja-Bruña et al. (2009, 2014) carried out an interpretation of the morphology and shallower structure of the study area and discussed the regional tectonic implications. Based on their study, we mostly focus on the active tectonic and sedimentary structures to gain insight into their tsunamigenic potential. The analysis of the geological and geophysical data is carried out in the three morphostructural provinces of the study area (Inset map in Figure 6): Venezuelan basin, Muertos margin, and Beata ridge.

5.3.1. Venezuelan Basin

The Venezuelan basin occupies the abyssal depths of the study area (i.e., >4,000 m of water depth) and is characterized by gentle seafloor slopes (Figure 6, Figure S2 in Supporting Information S1). The basin shows a layer of mostly pelagic sediments with a ≈1 sTWT-thick underlain by the igneous rocks of the CARIB LIP (Figures 7 and 8). The most distinct seafloor features are several isolated mounds, a zone with sediment waves, and the Muertos trough. The mounds are old features that rise 200–500 m above the surrounding seafloor and are the surface expression of basement highs of the CARIB LIP. Sedimentary waves are in the northwestern corner of the basin, with lengths of tens of km and amplitudes of up to 100 m (Figure 6). The evidence of tectonic deformation in the Venezuelan basin province is limited to the Muertos trough area (Figure 8). This trough is an elongated E─W depression reaching a water depth of 5,580 m, filled with horizontal turbidites yielding a flat seafloor, while the Venezuelan basin is filled by gentle northward dipping sediment beds. The Muertos depression is bounded in the north by the frontal thrust of the MTB, and in the south by a succession of bathymetric scarps. These scarps can reach 200 m in height, are progressively curved along the strike to the N, and disappear beneath the MTB (Figure 6). Seismic data show that these scarps are the surface expression of dip-slip normal faults trending sub-parallel to the trough (Muertos Trough Fault Zone, MTFZ in Figure 8). Faults produce offsets of 0.1–0.2 sTWT (≈100–200 m) in the sedimentary seismic horizons but locally also at the top of the basement (i.e., CARIB LIP). Faults are sub-vertical and have a preferential northward dipping in the Venezuelan basin and a southward dipping in the Muertos trough. Fault lengths are variable and are replaced along the strike in agreement with a step-over or relay extensional deformation pattern, but some segments reach 50–60 km in length. Faults can also be identified buried within the sedimentary horizons of the turbidite wedge of Muertos trough (Figure 8), suggesting no recent activity. These faults are only identifiable in the vicinity of the Muertos trough and were interpreted as a combination of the deformational response to tensile flexural stresses resulting from the bending of the interior of the CARIB plate that is overthrusted by the island arc, and to the differential along-strike overburden of the MTB (Granja-Bruña et al., 2009, 2014). The geological, seismological, and geodetic data

15252027, 2025, 6, Downloaded from https://agupubs.onlinelibrary.wiley.com/doi/10.1029/2024GC012092 by Universidad Complutense De, Wiley Online Library on [02/06/2025]. See the Terms and Conditions (https://onlinelibrary.wiley.com/terms-and-conditions) on Wiley Online Library for rules of use; OA articles are governed by the applicable Creative Commons License

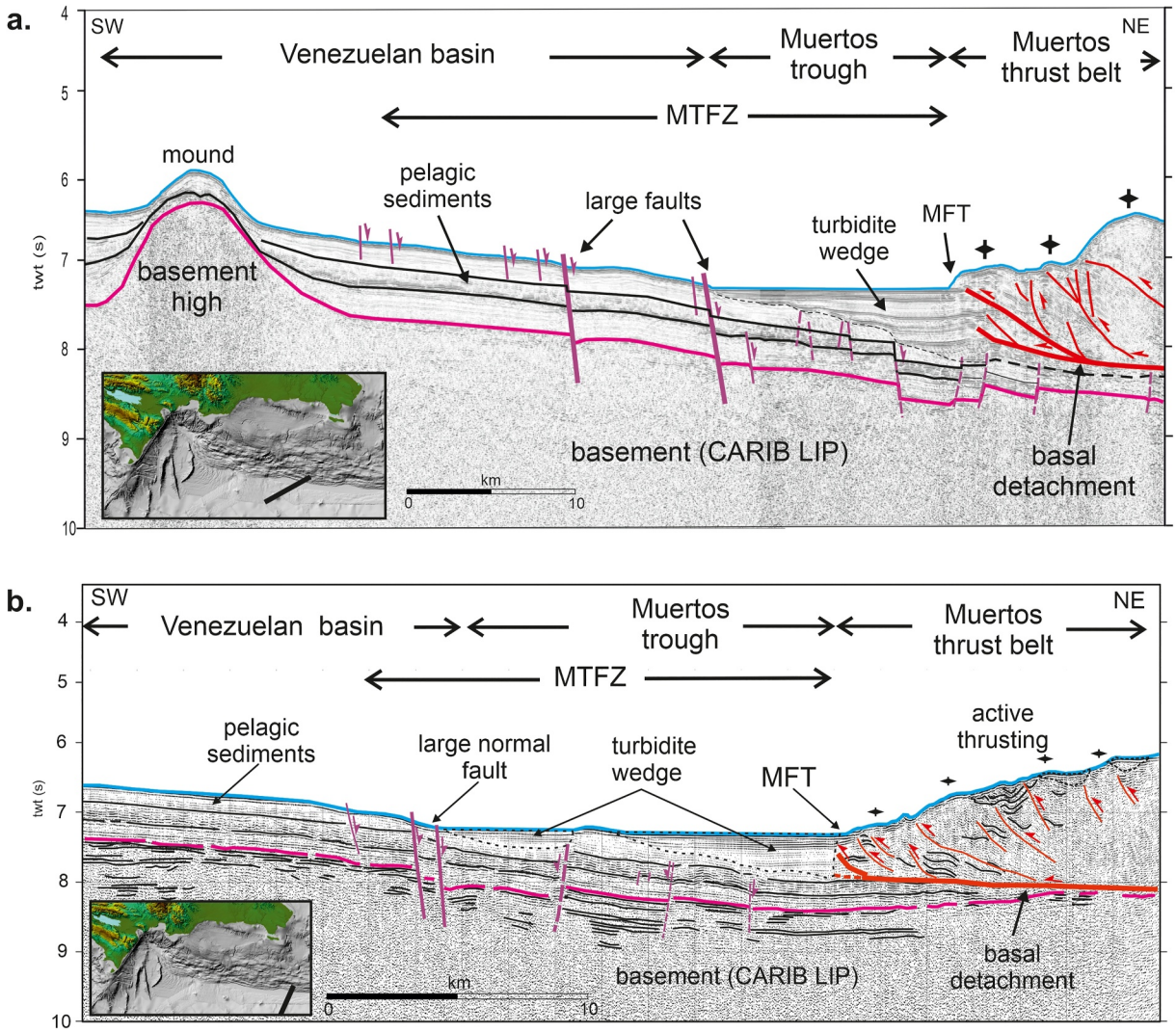

Figure 8. Line drawing interpretation of across-strike seismic sections showing Muertos trough fault zone (MTFZ). MFT: Muertos Frontal Thrust. See map inset for location. See legend of Figure 7 for details. (a) Profile in the western sector of the Muertos trough. (b) Profile in the central sector of the Muertos trough (modified from Granja-Bruña et al., 2009).

clearly indicate an active shortening along the Muertos margin. It is therefore reasonable to assume that some activity is occurring along some of these faults in the outer wall of the Muertos trough (MTFZ in Figure 8).

5.3.2. Muertos Margin

The regional structure of the Muertos margin shows a good structural analogy to active thrust belts and accretionary prisms around the world (Noda, 2016). The seafloor is mostly occupied by the contractional MTB that lies along the lower and middle margin slopes, while the upper margin is occupied by thick layers of slope sediments and the San Pedro basin (Figure 7). While the MTB represents the frontal region of an active imbricate system, the upper slope sediments and the San Pedro basin cover the distal part of the imbricate system as well as island arc basement terranes (Gorosabel-Araus et al., 2021). The upper slope then appears to be largely tectonically inactive (Figure 7).

5.3.2.1. Muertos Thrust Belt

The MTB shows a steep and stepped slope resulting from long-lived active folding and thrusting (Granja-Bruña et al., 2009, 2014, 2015). The overall surface expression of the MTB belt is characteristic of active contractional

15252027, 2025, 6, Downloaded from https://agupubs.onlinelibrary.wiley.com/doi/10.1029/2024GC012092 by Universidad Complutense De, Wiley Online Library on [02/06/2025]. See the Terms and Conditions (https://onlinelibrary.wiley.com/terms-and-conditions) on Wiley Online Library for rules of use; OA articles are governed by the applicable Creative Commons License

15252027, 2025, 6, Downloaded from https://agupubs.onlinelibrary.wiley.com/doi/10.1029/2024GC012092 by Universidad Complutense De, Wiley Online Library on [02/06/2025]. See the Terms and Conditions (https://onlinelibrary.wiley.com/terms-and-conditions) on Wiley Online Library for rules of use; OA articles are governed by the applicable Creative Commons License

imbricate systems showing an alternation of elongated troughs and anticline ridges (Figure S2 in Supporting Information S1). Ridges have variable size along the strike, and oriented sub-parallel to the compressive deformation front (Muertos frontal thrust, MFT in Figure 6) located to the toe of the margin slope. Most individual anticline ridges can be mapped along-strike for several tens of km and then replaced by other ridges by means of transfer zones showing an anastomosing geometry in map-view. Generally, the individual anticline ridges show a characteristic asymmetrical cross-section with a steeper forward limb in agreement with S-verging fault-propagation folds. The internal structure of the thrust belt is imaged by N-dipping reflectors, suggesting a prevailing S-verging structure of imbricate thrust sheets (Figure 7). The surface expression of the imbricate thrust sheets are fault-propagation folds (i.e., anticline ridges) and piggy-back basins (i.e., troughs). The MTB shows a dominant E─W orientation but the size is variable along the strike. The width decreases progressively eastward from 75 km to the south of Punta Palenque to 35 km to the south of the Mona passage (Figure 6). In the south of Punta Salinas, the surface expression of the thrust belt disappears beneath a steep insular slope, and the platform shelf. Westwards, at the base of the insular slope of Ocoa Bay, there are only two W─E trending anticline ridges. These ridges, as well as the onshore Sierra de Martín García (SMG in Figure 6) and the Bahoruco range, are flanked by roughly E─W trending thrust faults related to the NE─SW compression because of the indentation of the Beata Ridge against south-central Hispaniola (Escuder-Viruete et al., 2024; Hernaiz-Huerta et al., 2007).

Based on geological field work and onshore subsurface data in south-central Hispaniola as well as marine geophysical data in the nearby insular slope, the MTB continues onshore as the Peralta thrust belt (Figure 6; e.g., Granja-Bruña et al., 2014; Hernaiz-Huerta et al., 2007; Heubeck & Mann, 1991). Because of the indentation of the Beata ridge, the predominant E─W trending structure of the MTB is dragged and oroclinally folded. In the east of Ocoa Bay, the MTB is dragged to the north turning clockwise to a N─S orientation and north of Ocoa Bay it turns counterclockwise to a NW-SE orientation. Such oroclinal folding can be illustrated by the frontal thrust of the MTB that continues onshore along the San Juan Los Pozos Fault Zone (SJLPFZ in Figure 6), which is the frontal thrust of the Peralta thrust belt. The oroclinal folding of the MTB is accompanied by an extreme narrowing, uplifting, and finally exhumed as the Peralta thrust belt.

5.3.2.1.1. Muertos Frontal Thrust

The imbricate system is developed over a basal detachment that consists of a low-angle mega-thrust fault that accommodates the convergence between the island arc crust and the interior of the CARIB plate (CARIB LIP). The surface expression of the basal detachment is the MFT located at the base of the insular slope margin. The MFT shows a sinuous geometry along the strike showing an alternation of salients and recesses (S and R in Figure 6). This detachment is imaged as a seismic horizon along the contact between the top of the CARIB LIP having high-amplitude sub-horizontal reflectors and the base of the overlying imbricate system showing low-amplitude northward dipping reflectors (Figure 7). The basal detachment is a continuous fault that can be observed at least up to 25 km of distance northwards from the MFT. Assuming an average P-wave velocity of 2,500 m/s for the imbricate system materials, the basal detachment is a gentle surface dipping 8°–10° to the north. This detachment allows the development of a thin-skin imbricate system of the MTB against a backstop formed by island arc terranes (Gorosabel-Araus et al., 2021; Granja-Bruña et al., 2014).

5.3.2.1.2. Muertos Mega-Splay

Most individual anticline ridges can be mapped along-strike for several tens of km, but in the middle slope of the MTB, several larger anticline ridges are forming magnificent bathymetric escarpments (Figure 6). Locally, the ridges rise as much as 1000 m over the surrounding seafloor and the forward limb show slopes >20° (Figure S2b in Supporting Information S1). The well-preserved morphology of the escarpments along the strike and the frequent slope failures due to the ongoing over-steepening suggest that they are largely active structures and locally rupturing the seafloor. Seismic data show they are the surface expression of a large S-verging out-of-sequence thrust fault zone that can be traced along strike for 250 km of length (i.e., Muertos mega-splay, MMS in Figure 6 and Figure S2 in Supporting Information S1). The estimated fault geometry based on the dip of the seismic reflectors in the anticline back-limbs suggests landward-dipping planes between 10° and 14° (averaged). In analogy with other thrust belts (e.g., Nankai, Bangs et al., 2009; Moore et al., 2007), these mega-splay faults probably branch upward from the basal detachment breaking through the MTB. The low-angle splay faults become steeper upwards, reaching the surface in several minor splays or branches (Figure 7). The surface expression of the mega-splay faults strongly suggests a significant activity, and then together with the basal

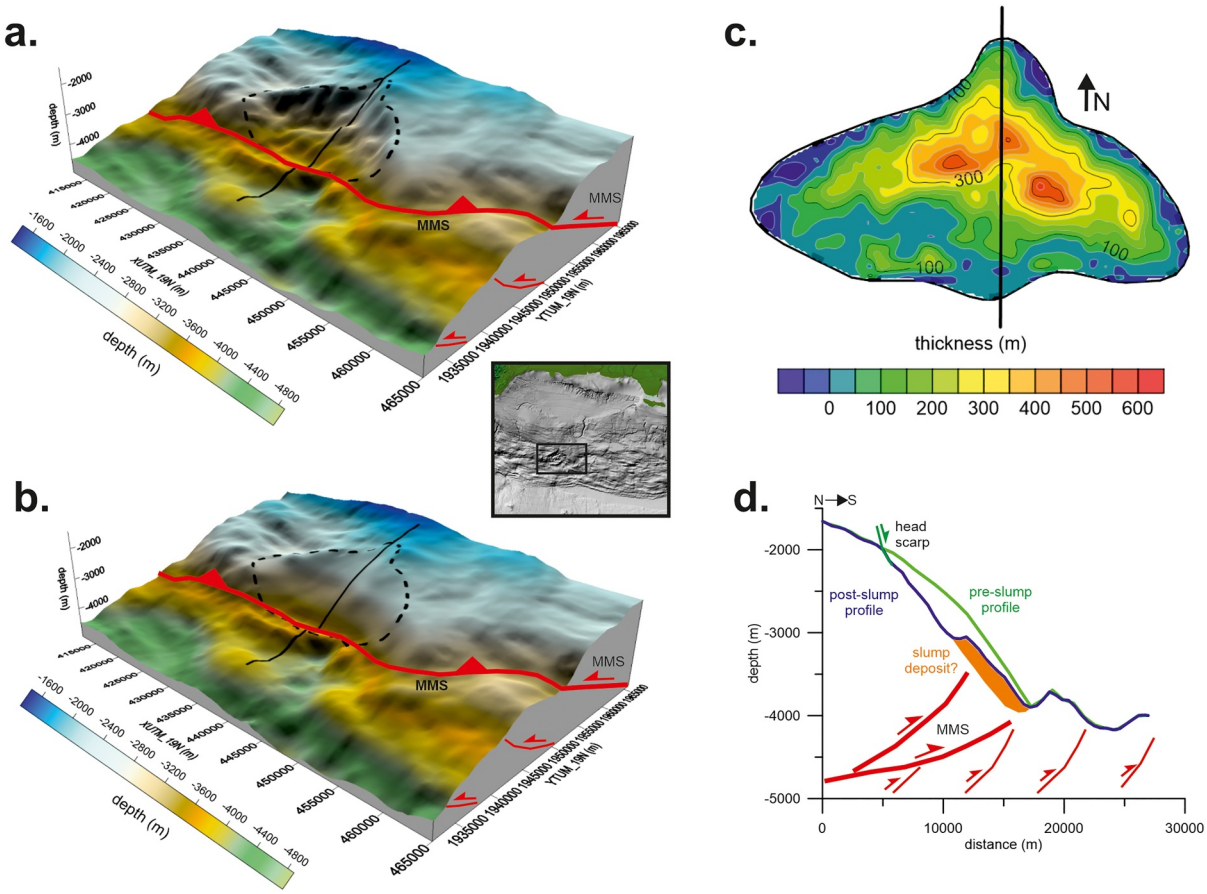

Figure 9. Color-shaded 3-D bathymetric image view from the SE of the Complutense slump. V.E. is 6×. MMS: Muertos Mega-splay. See map inset for location. (a) Pre-slump surface. (b) Post-slump surface. (c) Contour map showing the mobilized material (i.e., residual between the pre- and post-slice bathymetric surfaces). (d) Profile showing the pre- and post-slump bathymetry. See location in (a–c).

detachment, they play an important role in accommodating the elastic strain caused by the relative motion between the island arc and the interior of the CARIB plate (CARIB LIP).

5.3.2.1.3. Seafloor Over-Steepening and Slumping

The ongoing vertical growing of the imbricate system by means of active tectonics and sediment accumulation yields a general over-steepening of the taper-slope of the MTB (Granja-Bruña et al., 2009, 2014, 2015). This is an optimal setting for gravitational slumping across the entire MTB. Slumping is triggered by two main factors: progressive over-steepening during inter-seismic periods and strong coseismic shaking. While most slope failures are relatively minor, the larger ones occur along major thrust faults with local zones of increased over-steepening and large escarpments (Figure 6). The largest identified gravity failure is the Complutense Slump (CS) located along the steep bathymetric escarpment formed by the MMS (CS in Figure 6; Granja-Bruña et al., 2014). This slump is correlated with the local over-steepening slope caused by the MMS (Figure 9). The head scarp of the CS has a triangular shape and is 44 km long. The simple geometry of the head scarp without entrants could suggest a single event, but the data are not conclusive. In the slumped region, minor head scarps suggest local slope instabilities. At the base of the slumped area, seismic data do not show any slump deposits, suggesting that the CS could not be a recent event. The slumped area is about 240 km^2 with the head scarp located at 2,000 m and the base at about 4,000 m water depth. The inferred volume of removed material is ≈30 km^3 (Figure 9). Due to its location in the upper MTB far from flow sediment sources and the small height of the head scarp, the mobilized material has to be mostly low-deformed hemipelagic slope sediment beds (fine sand, silt and clay) with densities ranging from 1.7 to 2.3 g/cm^3. The runout is difficult to estimate because there is not clear evidence of the slump deposit, but it should be at least 5 km based on the post-slump bathymetry (Figure 9d).

15252027, 2025, 6, Downloaded from https://agupubs.onlinelibrary.wiley.com/doi/10.1029/2024GC012092 by Universidad Complutense De, Wiley Online Library on [02/06/2025]. See the Terms and Conditions (https://onlinelibrary.wiley.com/terms-and-conditions) on Wiley Online Library for rules of use; OA articles are governed by the applicable Creative Commons License

15252027, 2025, 6, Downloaded from https://agupubs.onlinelibrary.wiley.com/doi/10.1029/2024GC012092 by Universidad Complutense De, Wiley Online Library on [02/06/2025]. See the Terms and Conditions (https://onlinelibrary.wiley.com/terms-and-conditions) on Wiley Online Library for rules of use; OA articles are governed by the applicable Creative Commons License

5.3.2.2. Upper Insular Slope

The main physiographic feature of the upper insular slope is the E–W trending bathymetric depression named San Pedro basin (SPB in Figure 6). The sediment beds of this basin extend over the upper margin slope burying the rear zone of the MTB and the island arc terranes (Figure 7). This depression is mainly bordered by structural highs (Figure 6): in the north by the San Pedro escarpment (SPE), in the south by an WNW–ESE trending Punta Palenque high (PPH), and in the south by the Saona ridge (SR).

5.3.2.2.1. San Pedro Escarpment

The surface expression of the SPE is an NNW–SSE trending slope between the shelf edge and the SPB seafloor bottom (Figure 6). The slope is incised by a dense canyon network flowing southward into the SPB and small gravity failures. Although this zone lacks high-resolution swath bathymetry coverage, the GEBCO 30 arc-sec gridded data enables us to map this escarpment for approximately 50 km along the strike. The escarpment shows a central sector with a steep slope where it reaches a maximum height of ≈1,000 m and it becomes gentle and fades up along strike. Seismic data do not show vertical offset between the sediment beds of the island shelf and the SPB, suggesting no recent deformation by faulting (Figure 10). To the east and south of Catalina Island (CI in Figure 6), there is a ≈W–E trending ridge, but seismic data are not conclusive about its origin, whether it is a structural ridge or an old reef knoll built up ringing the island shelf (Figures 10c and 10d). Locally, the platform seafloor and the slope are deformed by growth and gravity-driven faults, but they are superficial and do not appear to be correlated with a deep-seated large fault along the SPE (Figures 10c and 10d). The origin of this escarpment was suggested to be associated with the offshore extension of the old Hispaniola fault zone (HFZ in Figure 6; Granja-Bruña et al., 2014). However, high-resolution marine data coverage does not reach the coast making difficult the onshore-offshore correlation.

5.3.2.2.2. Saona Ridge

The surface expression of the Saona ridge is a WSW–ENE trending feature, with an asymmetrical cross-section bathymetry having an N-facing scarp and an S-facing smooth slope (SR in Figure 6). The scarp rises to a maximum height of ≈500 m in the eastern sector over the seafloor of the SPB (Figure 11c). The scarp is observable for 60 km along the strike and progressively fades to the NE in the vicinity of Saona Island and to the W beneath the sediments of the SPB. This ridge is the surface expression of an uplifted and faulted block that separates the ponded sediment fill of the SPB from southward-tilted slope sediment layers covering the MTB. The ridge was interpreted to be the result of a left-lateral transpressive fault based on the stratigraphical correlation between the SPB and the slope sedimentary layers (Figure 11, Gorosabel-Araus et al., 2021). Therefore, the southward-tilted slope layers could be considered as the seaward continuation of the SPB. Assuming this interpretation, the transpressive structures rooting the Saona ridge have been inactive since the Middle Miocene. The ridge and its flanks are dominated by shallow faults and gravity instabilities and landslides (See yellow stars in Figure 6).

5.3.2.2.3. Punta Palenque High

The Punta Palenque high is a wide bathymetric elevation that separates the ponded depression of the actual San Pedro Basin from the steep slope of the active MTB (PPH in Figure 6). Seismic data show that this high is formed by a thick sequence of sedimentary beds originating in the SPB that were burying the rear of the imbricate structure. The origin of this high is related to the landward and vertical growth of the MTB (Granja-Bruña et al., 2014). Most of the buried imbricate structure beneath the Punta Palenque high seems to have low activity, but some of these thrusts form a fault-propagation fold structure that deforms the seafloor, suggesting local recent activity (Muertos rear thrust, MRT in Figures 6 and 12).

The seaward slope of the Punta Palenque high shows a seafloor characterized by widespread sub-parallel scarps of tens of meters in height and several tens of km in length (Figure 6). These scarps are controlled by active bending-moment normal faulting (gravity-driven) arranged in an echelon. These faults are the deformational response to the ongoing growth of the thrust belt and the consequent over-steepening of the slope (i.e., gravity-driven; Granja-Bruña et al., 2014). Those faults are locally crossed by incised channels flowing into the MTB (Figure 6). The landward slope of the Punta Palenque high shows a gentle seafloor slope characterized by local gravity sliding and incised channels flowing into the SPB.

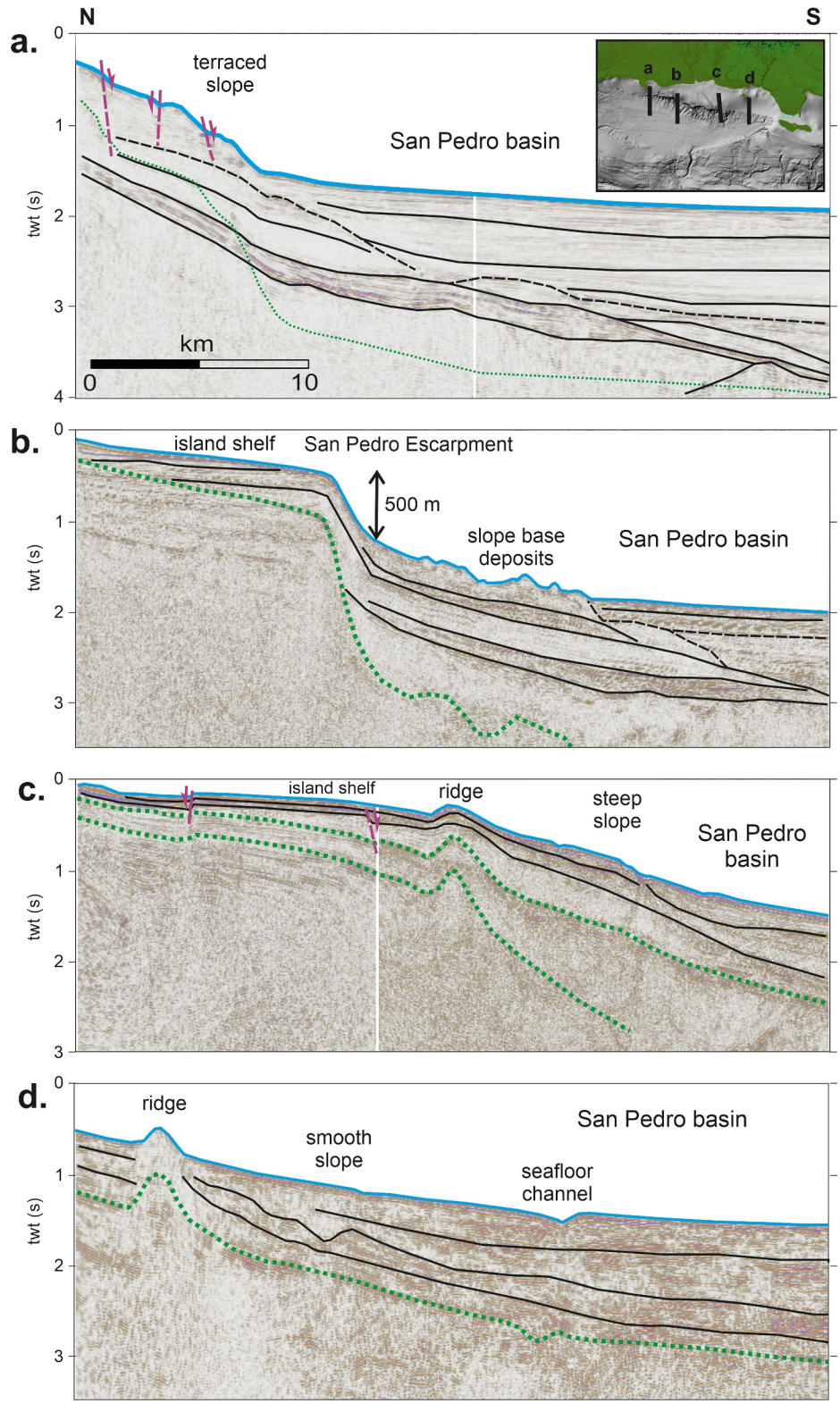

Figure 10. Line drawing interpretation of four across-strike seismic sections showing the San Pedro escarpment. See legend of Figure 7 for details.

15252027, 2025, 6, Downloaded from https://agupubs.onlinelibrary.wiley.com/doi/10.1029/2024GC012092 by Universidad Complutense De, Wiley Online Library on [02/06/2025]. See the Terms and Conditions (https://onlinelibrary.wiley.com/terms-and-conditions) on Wiley Online Library for rules of use; OA articles are governed by the applicable Creative Commons License

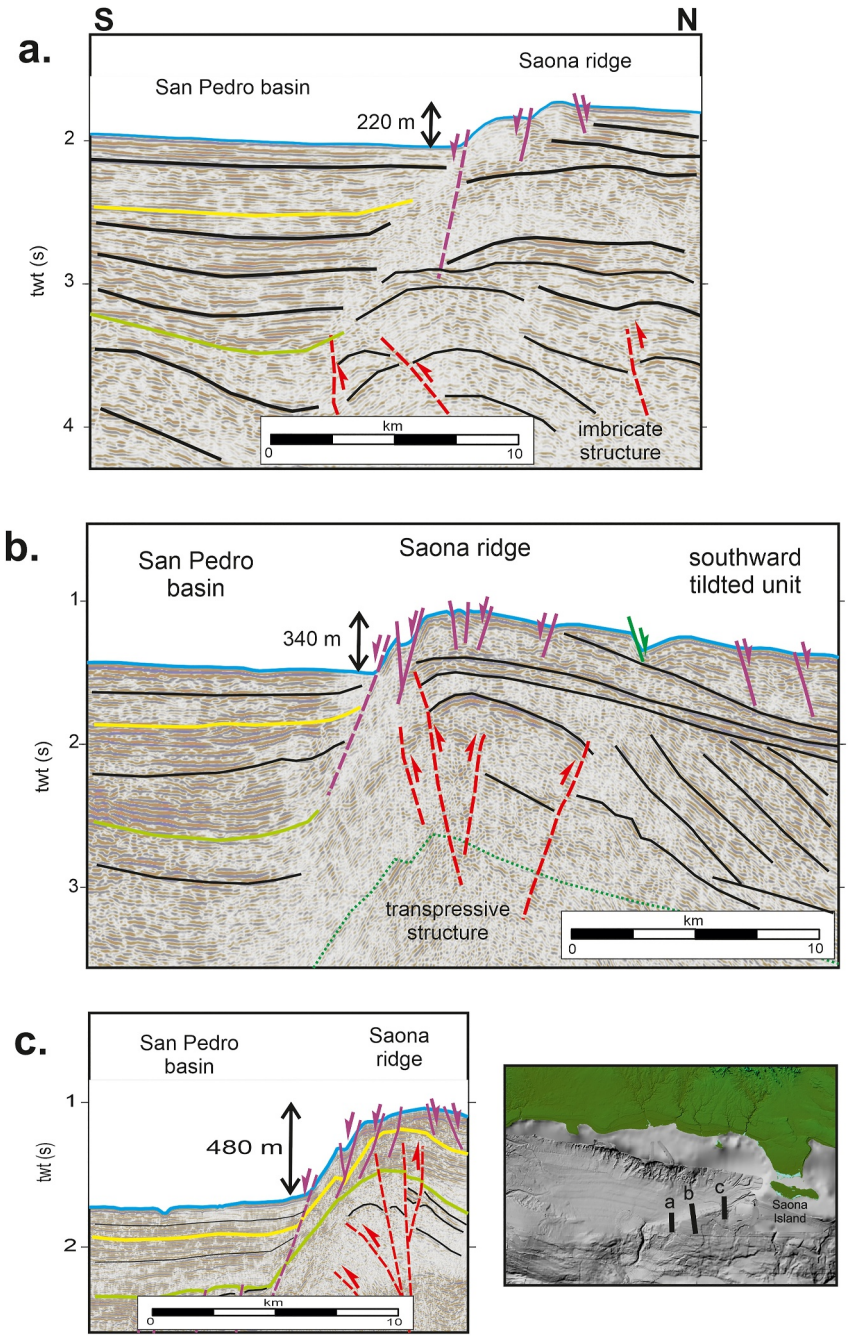

Figure 11. Line drawing interpretation of across-strike seismic sections showing the Saona ridge. See the inset map for location. Top Miocene and Top Middle-Miocene horizons are shown in yellow and green, respectively (modified from Gorosabel-Araus et al., 2021). See legend of Figure 7 for details.

5.3.2.3. Punta Salinas Slope

South of Ocoa Bay and Punta Salinas, the Muertos margin is replaced by a steep slope and the island shelf (Figure 6). The slope is incised by a dense canyon system flowing from the island shelf. At the base of the slope there is a WNW–ESE trending narrow compressive belt deforming the Muertos trough turbidites (See Figure 9 in Granja-Bruña et al., 2014). The turbidites being actively folded that suggest active compressive stresses between the island arc crust and the Beata ridge indenter. This island shelf is very shallow (<100 m of water depth) almost flat and has variable seaward extension. Seismic data show that the platform is formed by flat and gently dipping

15252027, 2025, 6, Downloaded from https://agupubs.onlinelibrary.wiley.com/doi/10.1029/2024GC012092 by Universidad Complutense De, Wiley Online Library on [02/06/2025]. See the Terms and Conditions (https://onlinelibrary.wiley.com/terms-and-conditions) on Wiley Online Library for rules of use; OA articles are governed by the applicable Creative Commons License

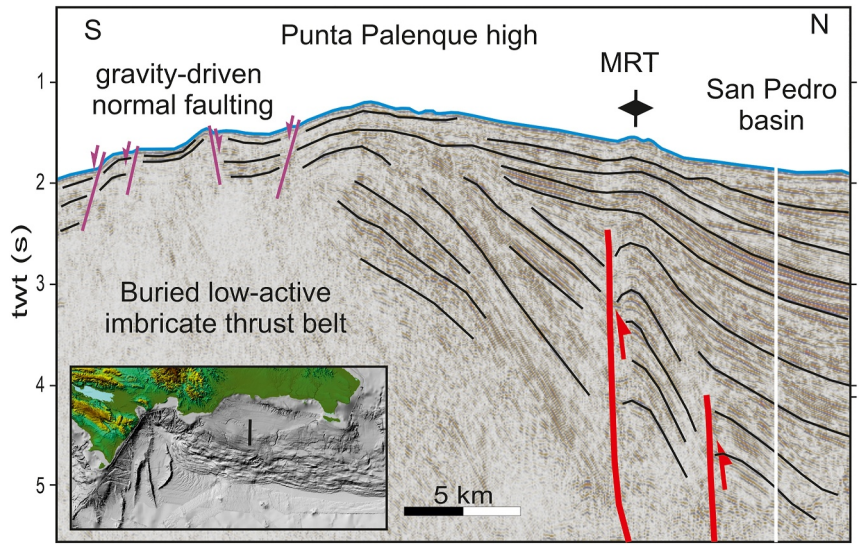

Figure 12. Line drawing interpretation of across-strike seismic sections showing the Punta Palenque high. See the inset map for location. See legend of Figure 7 for details. Note the fold-propagation fault deforming the seafloor of the San Pedro basin (Muertos Rear Thrust, MRT).

sediment beds of variable thickness laying unconformably over the MTB (Figure 13). Imbricate structures can be seismically imaged beneath the flat platform verging to the west. The orientation of the MTB rapidly changes from roughly W–E in the offshore to N-S in the Punta Salinas-Ocoa Bay. The frontal thrust of the offshore MTB follows an N–S canyon along the slope and the eastern side of Ocoa Bay. This structure can be correlated with the

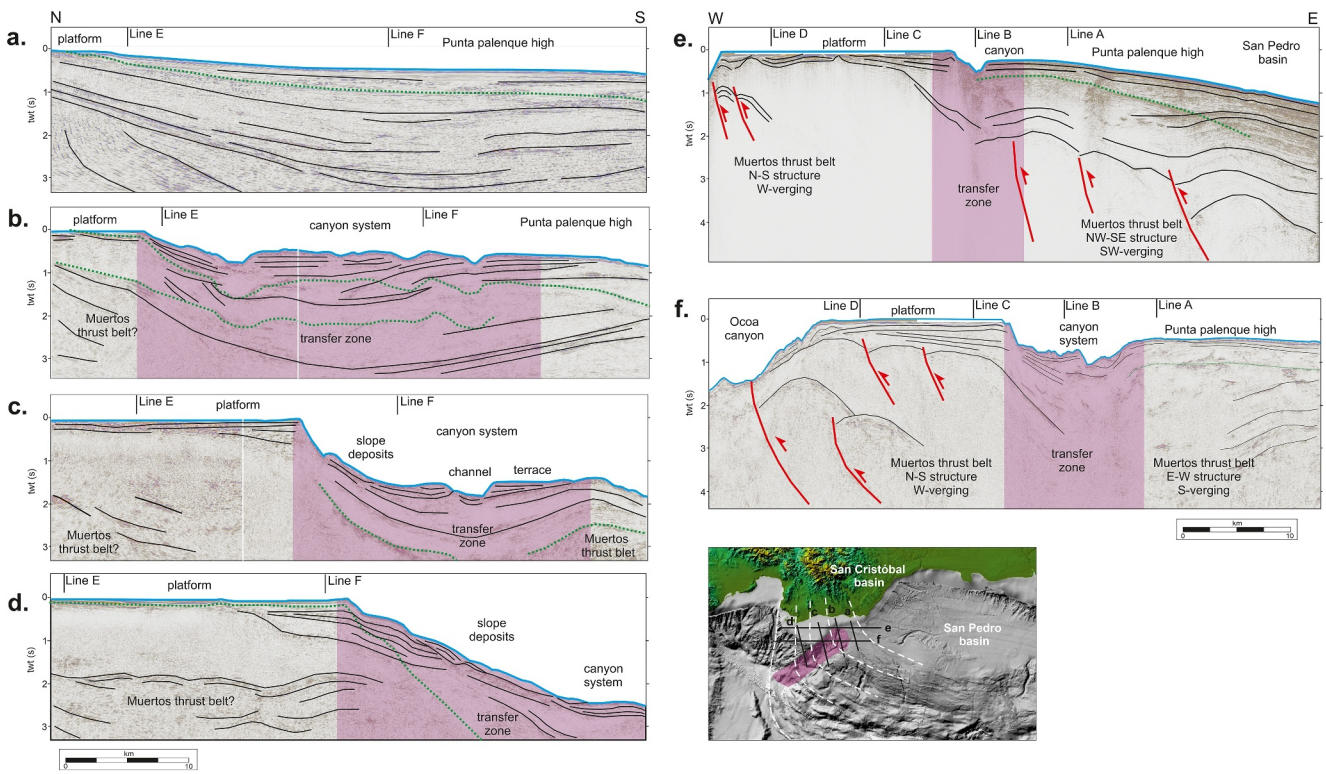

Figure 13. Line drawing interpretation of across-strike seismic sections showing the Punta Palenque canyon system. See legend of Figure 7 for details. See the inset map for location. The pink region shows the Punta Palenque canyon system. Dashed white lines in the map show the turn in the orientation of the structural trends of the imbricate structure of the MTB.

15252027, 2025, 6, Downloaded from https://agupubs.onlinelibrary.wiley.com/doi/10.1029/2024GC012092 by Universidad Complutense De, Wiley Online Library on [02/06/2025]. See the Terms and Conditions (https://onlinelibrary.wiley.com/terms-and-conditions) on Wiley Online Library for rules of use; OA articles are governed by the applicable Creative Commons License

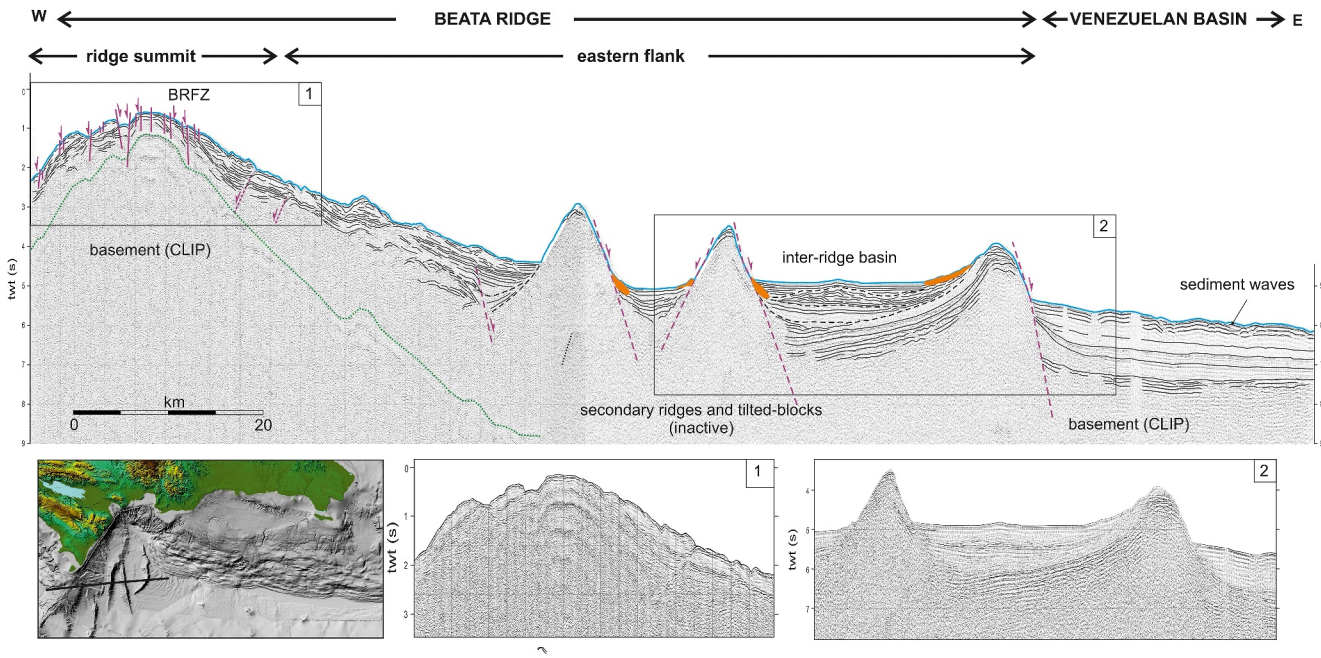

Figure 14. Line drawing interpretation of a regional across-strike seismic section of the Beata ridge (modified from Granja-Bruña et al., 2014). V.E. is 6.6× on the seafloor. See the inset map for location. See legend of Figure 7 for details. Insets show enlarged sectors of; 1) Summit fault zone (BRFZ), 2) and secondary ridges and intra-ridge basin.

onshore San Juan-Los Pozos Fault Zone, which is the frontal thrust of the Peralta thrust belt (Hernaiz-Huerta et al., 2007; Heubeck & Mann, 1991).

In the upper slope margin, the transition between the Muertos margin and the Punta Salinas region takes place along a NE-SW oriented canyon system (Figure 6). The system flows from the platform edge and the summit of the Punta Palenque high and ends downslope in the imbricate structure of the active MTB. This drainage system is very incised and locally reaches a width of 8 km. At some points, there is almost 800 m of height between the platform edge and the seafloor of the canyon. Seismic data are not conclusive regarding an offset that can be ascribed to individual faults (Figure 13). A locally steep slope with small tributary canyons and slump deposits at their base in the canyon floor suggests dominant erosional processes (Figure 6).

Northeastwards of the Punta Palenque high, the canyon system disappears, and the seismic lines show continuous sedimentary beds of the San Pedro basin and the onshore San Cristobal basin with no deformation by faulting. The curved and sinuous shape of the canyon could suggest that it is not tracing a deeper fault (inset map in Figure 13). A more plausible interpretation for the origin of this canyon system is that it is formed along a transfer zone allowing a sharp transition between the active MTB and the stable Punta Salinas region. This transfer zone would facilitate the MTB structural reorganization to accommodate the oroclinal folding, narrowing, and uplifting of the MTB because of the impingement of the Beata indenter. In the transfer zone, the deformation is diffuse, which would be favorable for the nucleation and subsequent development of local erosional features.

5.3.3. Beata Ridge

The Beata ridge consists of a bathymetric high in the interior of the CARIB plate whose tectonic origin is not well understood. Sampling and seismic refraction experiments suggested that the Beata ridge is part of the CARIB LIP (e.g., Driscoll & Diebold, 1999; Mauffret & Leroy, 1999; Mauffret et al., 2001). The ridge has no significant seismic activity (Figure S1a in Supporting Information S1) and shows a highly asymmetrical E–W bathymetric profile where the eastern flank is significantly wider and less steep than the western flank (Figures 6 and 14).

The eastern flank shows a slope consisting of alternating ≈N–S trending secondary ridges and troughs (Figure 14). The secondary ridges reach a length of 70 km, have steep sides, and rise as much as 1,600 m above the surrounding seafloor. The stratigraphical analysis of the adjoining troughs filled by sediments suggests that the

15252027, 2025, 6, Downloaded from https://agupubs.onlinelibrary.wiley.com/doi/10.1029/2024GC012092 by Universidad Complutense De, Wiley Online Library on [02/06/2025]. See the Terms and Conditions (https://onlinelibrary.wiley.com/terms-and-conditions) on Wiley Online Library for rules of use; OA articles are governed by the applicable Creative Commons License

15252027, 2025, 6, Downloaded from https://agupubs.onlinelibrary.wiley.com/doi/10.1029/2024GC012092 by Universidad Complutense De, Wiley Online Library on [02/06/2025]. See the Terms and Conditions (https://onlinelibrary.wiley.com/terms-and-conditions) on Wiley Online Library for rules of use; OA articles are governed by the applicable Creative Commons License

ridges are fault-controlled basement blocks, but the deformation ceased between Lower Miocene and Pliocene times (Granja-Bruña et al., 2014). Northwards, the secondary ridges fade progressively beneath the sediments and the eastern flank of Beata Ridge and the eastern margin of the Bahoruco peninsula.

The summit of the Beata ridge mainly consists of a band of ≈10 km wide stepped seafloor showing a succession of bathymetric scarps and structural lineaments-oriented NNE–SSW (Figures 6 and 14). These features were interpreted as the surface expression of numerous normal faults formed by an active NW–SE oriented extension (Beata ridge fault zone, BRFZ in Figure 6). Faults offset the seafloor forming west- and east-facing bathymetric scarps, which extend tens of km along the strike and reach heights of 250 m (Figure 14). In map-view fault segments seem to be connected along strike by transfer or relay/step-over zones. This fault zone continues northeastward forming minor NNE–SSW trending steps disrupting the canyon network developed along the eastern Bahoruco slope. This slope was interpreted as the surface expression major NE–SW-trending SE-dipping normal fault. This fault is responsible for the straight morphology of the eastern coast of the Bahoruco Peninsula and is interpreted as an old tear fault that accommodates the sharp transition from thrusting at the Muertos margin to collision and uplifting in the Bahoruco peninsula and adjacent areas (Granja-Bruña et al., 2014). Recent studies in the south-central Dominican Republic interpreted a Pleistocene left-lateral strike-slip fault onshore along the western Ocoa Bay continuing southward along the coast of the Bahoruco slope (Escuder-Viruete et al., 2023). However, offshore data do not show any evidence of recent activity in this fault except for some minor gravity-driven shallow faults disrupting locally the canyon network (Figure 6).

The western flank, known as the Beata escarpment, is the result of a major NW-dipping normal fault that offsets the thick CARIB LIP crust of the Beata ridge (≈4,300 m) from the thin crust of the Haiti sub-basin (Driscoll & Diebold, 1999). This escarpment shows an incised canyon network disrupted by minor faults driven by gravitational forces because of the steep slope (Figure 6). Slopes vary between 8.5° and 11.5°, with locally higher slopes of 20° related to highly incised canyons, but there is no evidence of slumping (Figure S2b in Supporting Information S1). Northwards, the western flank is replaced by the western Bahoruco slope that connects the Bahoruco peninsula with the Haiti sub-basin seafloor. On the northern edge of the sub-basin, a buried wedge of highly deformed sediments through S-verging thrust faults was identified, but this system is currently inactive (Granja-Bruña et al., 2014).

6. Discussion and Tsunami Source Characterization

The integration of seismotectonic, structural, and morphological data and the combined interpretation allow us to identify and characterize the tsunamigenic tectonic and landslide features in the southern offshore Dominican Republic. From the size, geometry, and rupture mechanism data of the tectonic sources, it is possible to estimate the magnitude of potential maximum seismic events using semi-empirical relationships (Wells & Coppersmith, 1994). The geometrical characteristics and parameters of the potential tectonic sources have been simplified to provide an initial assessment and streamline the calculation process. The size of the earthquake generated by each fault segment is represented by the size of the rectangle (Figure S3 in Supporting Information S1). In accordance with our source characterization, we have obtained earthquake magnitudes ranging from Mw 5.6 to 8.1 (Table 1). The maximum length of individual sources varies from 20 km for the smallest rupture (small segment of the BRFZ) to 300 km for the largest one (MFT).

6.1. Muertos Trough Fault Zone (MTFZ)

The well-preserved bathymetric expression of the normal fault scarps along the outer wall of the Muertos trough suggests recent activity. The extensional driven mechanism in the MTFZ is active because of the N-S shortening between the CARIB LIP and the island arc along the Muertos trough. This mechanism is analogous to the deformation mechanism in the outer rise of active subduction zones (Granja-Bruña et al., 2009 and therein references). The flexural bending of the incoming plate creates or reactivates normal faults, some of them of crustal scale where significant earthquakes are nucleated. However, the Mw > 4.5 seismicity in the Muertos trough is scarce and disperse (Figure 4, Figure S1a in Supporting Information S1), suggesting that deformation is mainly aseismic and/or with small magnitudes. The CMT catalog only provides one focal mechanism in this region occurred in 1989 with Mw 5.4 showing an oblique normal rupture (Label 061889A in Figure S1b in Supporting Information S1). This mechanism shows nodal planes trending NW–SE and NE–SW and a focal depth of 73 km. The nodal planes are then very oblique relative to the E–W orientation of the MTFZ. The focal depth is

Table 1
Tsunami Source Parameters

Scenario	Lat (°)	Lon (°)	Strike (°)	Dip (°)	Rake (°)	Length (km)	Width (km)	RA (km^2)	L/W	Fault type	Mw (SRL)	Mw (RW)	Mw (RA)	Mw (averaged)
MTFZ*	17,1	−68,9	100	80	90	170	16	2,720	10,6	normal	7,8	6,6	7,4	7,3
MTFZ	17,1	−68,9	100	80	90	60	6	360	10	normal	7,2	5,7	6,5	6,5
MFT*	18	−69,4	100	10	90	300	85	25,500	3,5	reverse	8	8,1	8,3	8,1
WMFT	18	−70	90	10	90	90	50	4,500	1,8	reverse	7,4	7,7	7,6	7,6
EMFT	18	−68,7	130	10	90	60	40	2,400	1,5	reverse	7,2	7,5	7,4	7,4
MMS*	18	−69,7	99	14	90	250	60	15,000	4,2	reverse	7,9	7,8	8,1	7,9
WMMS	18	−70	105	14	90	130	40	5,200	3,3	reverse	7,6	7,5	7,7	7,6
EMMS	18	−69,2	105	14	90	130	40	5,200	3,3	reverse	7,6	7,5	7,7	7,6
MRT	18	−69,7	110	60	90	35	6	210	5,9	reverse	6,9	5,9	6,4	6,4
BRFZ*	17,3	−71,6	40	80	90	90	2	180	45	normal	7,4	4,7	6,2	6,1
BRFZ	17,3	−71,6	40	80	90	20	2	40	10	normal	6,6	4,7	5,6	5,6
CS	17,6	−69,6												

Note. Geographical coordinates in WGS84. (*) Worse-case scenario. MTFZ: Muertos trough fault zone. MFT: Muertos Frontal Thrust. MRT: Muertos Rear Thrust. WMFT Western Muertos Frontal Thrust. EMFT: Eastern Muertos Frontal Thrust. MMS: Muertos Mega-splay. WMMS: Western Muertos Mega-splay. EMMS: Eastern Muertos Mega-splay. BRFZ: Beata Ridge Fault Zone. CS: Complutense slump (Volume of ≈30 km^3). SLR: Surface Rupture Length. L/W: length/Width ratio. RA: Rupture area. RW: Rupture Width. Mw: Moment magnitude (Wells & Coppersmith, 1994).

too large to be linked to a rupture of the CARIB LIP because the thickness crust ranges only ≈14–18 km (Nuñez et al., 2019). Both last two observations related to this event are incompatible with a rupture in the MTFZ. However, because of the large size and clear seafloor expression, the MTFZ could be considered as a potential tsunamigenic source. A worst-case scenario with a complete rupture of the CARIB LIP crust (16 km-thick) along the MTFZ would imply a rupture length of 170 km that could generate a Mw 7.3 event (Figure 15, Table 1. Figure S3e in Supporting Information S1). A more feasible scenario would involve a rupture along individual segments of larger faults with a rupture length of 60 km. Assuming a fault width of 6 km based on the interpretation of the seismic sections, it could generate Mw 6.5 events (Table 1. Figure S3f in Supporting Information S1). If the rupture reaches the seafloor as observed in the seismic data, the MTFZ would have significant tsunamigenic potential.

6.2. Muertos Thrust Belt (MTB)

The seismogenic zone in the MTB with magnitudes above 4.5 is completely offshore, entailing a tsunami threat to the southern Dominican Republic. Because of their shallower focal depth, the events of the Muertos Shallow sub-group are potentially tsunamigenic during a strong event that could yield a rupture/deformation on the seafloor. The events of the Muertos Deep Sub-group also have significant magnitudes, but they are much deeper and are probably unlikely to rupture on the seafloor. There is no documented seafloor deformation and tsunamis related to the events of the Muertos Group, but a potential strong shaking close to the steep offshore areas could trigger submarine landslides causing tsunamis.

Many thrust faults in the MTB reach the seafloor or just below the seafloor deforming the surface, but the length of most of them is relatively modest (i.e., few tens of km) and therefore have a limited coseismic tsunamigenic potential. However, the MFT and the MMS deform the seafloor (Figure 7). A big rupture along these structures could yield significant seafloor deformation with high tsunamigenic potential. The location, size, geometry and strike of the MFT and MMS strongly suggest that these faults are related to the reverse focal mechanism of the Muertos Shallow Group in the SPB region (Events 1, 2 and 3 with magnitudes 5.3–6.7 and depths 15–16 km in Figure 4). These types of events are common in compressional settings such as subduction zones and fold-and-thrust belts and are related to the events nucleated both in the basal detachment and large thrust faults into the compressive thrust belt (e.g., Stern & Gerya, 2018). In such cases, the earthquake fault is frequently the low-angle plane dipping to the hinterland. In addition, the continuous non-seismic deformation in the overall thrust belt

15252027, 2025, 6, Downloaded from https://agupubs.onlinelibrary.wiley.com/doi/10.1029/2024GC012092 by Universidad Complutense De, Wiley Online Library on [02/06/2025]. See the Terms and Conditions (https://onlinelibrary.wiley.com/terms-and-conditions) on Wiley Online Library for rules of use; OA articles are governed by the applicable Creative Commons License

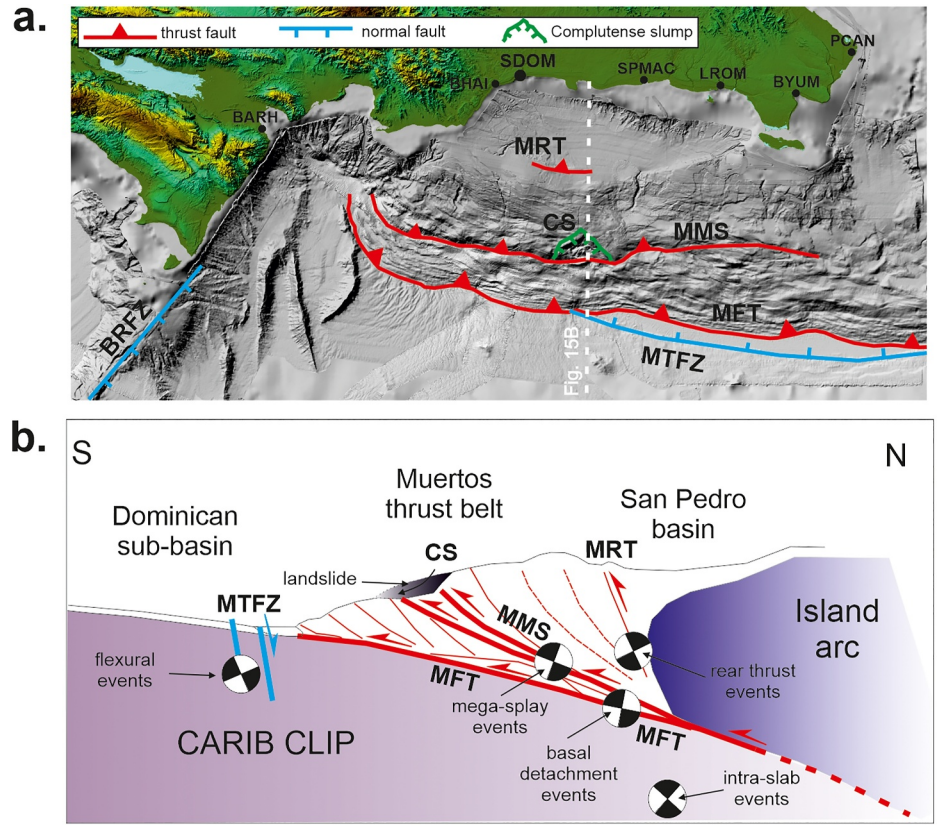

Figure 15. Potential tsunami sources. MFT: Muertos Frontal Thrust. MMS: Muertos Mega-splay. MRT: Muertos Rear Thrust. CS: Complutense slump. MTFZ: Muertos Trough Fault Zone. BRFZ: Beata Ridge Fault Zone. (a) Map-view of the tsunami sources. Most populated cities along the south coast. BARH: Barahona. BHAI: Bajos de Haina. SDOM: Santo Domingo. SPMAC: San Pedro de Macorís. LROM: La Romana. BYUM: Boca de Yuma. PCAN: Punta Cana. (b) Conceptual cross-section of the Muertos margin. See location in (a).

resulting in the growing of the anticline ridges yields an overstepping of the seafloor slope. This circumstance is favorable for gravitational slumping that can also be triggered by the shaking during large seismic events.

6.2.1. Muertos Frontal Thrust Belt (MFT)

The MFT is a first order active thrust fault that some authors speculated that it could rupture its entire length from Hispaniola to Puerto Rico, yielding an Mw 8.0 event (e.g., McCann, 2006). Historical records are not conclusive as to whether this first-order fault had produced the Mw 8.0 1751 earthquake in central southern Hispaniola (ten Brink et al., 2011). The northward extension of the MFT up to 25 km should be considered as a minimum value because of the limited resolution and penetration of the seismic reflection data in the deep internal region of the MTB. The tsunamigenic potential of the MFT is currently uncertain, but rupturing the entire length is likely improbable. Swath bathymetry shows that the MFT is segmented along the strike, which could limit the maximum rupture length during a seismic event. This segmentation of the MFT is interpreted from the along-strike alternation of broad salients and narrow recesses (R and S, respectively, in Figure 6). The recesses were interpreted as a result of the thrusting of basement highs and seamounts, yielding tectonic erosion and damaging the imbricate structure of the thrust belt (Granja-Bruña et al., 2009, 2014). These thrusted features act as tectonic asperities that generate or impede megathrust earthquakes and it depends on their relative locations to the earthquake nucleation zone defined by depth variable friction parameters (Wang & Bilek, 2011; Yang et al., 2012). One scenario is that the thrusted highs act as asperities segmenting the MFT that could limit the maximum length of the fault segments to be broken during an event, and another scenario is that these asperities favor megathrust earthquakes on the MFT that can nucleate at shallow depths and rupture the entire seismogenic zone. The worst-case scenario would be the complete rupture of the MFT between the Mona Passage in the east to the Beata ridge in the west along

15252027, 2025, 6, Downloaded from https://agupubs.onlinelibrary.wiley.com/doi/10.1029/2024GC012092 by Universidad Complutense De, Wiley Online Library on [02/06/2025]. See the Terms and Conditions (https://onlinelibrary.wiley.com/terms-and-conditions) on Wiley Online Library for rules of use; OA articles are governed by the applicable Creative Commons License

15252027, 2025, 6, Downloaded from https://agupubs.onlinelibrary.wiley.com/doi/10.1029/2024GC012092 by Universidad Complutense De, Wiley Online Library on [02/06/2025]. See the Terms and Conditions (https://onlinelibrary.wiley.com/terms-and-conditions) on Wiley Online Library for rules of use; OA articles are governed by the applicable Creative Commons License

320 km (MFT in Figure 15, Table 1. Figure S3a in Supporting Information S1). The geometry of the rupture would be assumed to be a plane oriented 100° and dipping 8º–10° toward the N, with a width of 70 km based on the gravity modeling and receiver functions (Granja-Bruña et al., 2010; Kumar et al., 2020). Assuming a pure reverse motion, this rupture area can generate an Mw 8.1 event. However, if we consider a more feasible scenario limiting the rupture size to the maximum length of the segments associated with the four salients between 60 and 90 km of length (R and S, respectively, in Figure 6), they could produce Mw 7.2–7.5 events (Table 1. Figure S3b in Supporting Information S1). Therefore, many of the scenarios for the MFT have a significant tsunamigenic potential.

6.2.2. Muertos Mega-Splay (MMS)

The Muertos mega-splay (MMS) shows continuity for 250 km along the strike with only local anastomosing zones suggesting minor segmentation. The absence of significant segmentation suggests that it could be more prone to a rupture along its entire length. Similar structures have been documented in the well-studied compressive margin of Nankai (Japan), where those large out-of-sequence thrusts were interpreted as mega-splay thrust faults with a high level of tsunami generation (e.g., Moore et al., 2007). The worst-case scenario would be a complete rupture along a main out-of-sequence strand (splay) between the Mona Passage in the east and the Beata ridge in the west. The geometry of the rupture would be assumed to be a plane oriented 100° and dipping 10° to the N, with an area of 250 km-long x 60 km-wide (MMS in Figure 15, Table 1. Figure S3c in Supporting Information S1). Assuming a pure reverse motion, this rupture area can generate an Mw 7.9 event. The rupture of the 1751 event could also be attributed to the MMS because of its location and size. ten Brink et al. (2011) suggested that the rupture of 1791 was in the eastern termination of the EFZ, but they also noticed that Muertos thrust faults also fit with their data. However, if we consider a more feasible scenario limiting the rupture size to the maximum length of 130 km, they could produce Mw 7.5–7.6 events (Table 1, Figure S3d in Supporting Information S1). Therefore, many of the scenarios for the MMS have a significant tsunamigenic potential.

6.2.3. Complutense Slump (CS)

The landslide tsunami sources would be characterized by a relatively large submarine slump that, if this volume is mobilized in one single and quick event, could generate tsunamis. Most of the gravity failures in the study area show a relatively small size, widespread minor slumping, and head scarps controlled by the sequential sliding process, and they initially have small tsunamigenic potential/threat. Because of its large size and location close to the active MMS, the CS could be considered as a feasible scenario for landslide tsunami sources in the southern Dominican Republic (Figure 9). Data are not conclusive if this slump was generated by a single event or is a result of a recurrent process of small slumping. However, assuming a worst-case scenario if this large gravity instability takes place as a single and quick event because of the progressive deformation and/or quick co-seismic deformation, it could generate a significant tsunami (Figure S3h in Supporting Information S1). CS seems to be an old feature, but it should be considered for worse-case tsunami simulation to assess the threat in the southern Dominican Republic.

6.3. Upper Muertos Insular Slope

A common characteristic of the potential sources located in the upper zone is their proximity to the coast (≈60 km), which results in a short time (5 min) of response in case of a tsunami. However, the sources identified here show in general low tsunami potential from expected seafloor rupture and/or tectonic deformation. This zone is characterized by overall shallow extensional tectonics with structures that reach unlikely seismogenic depths. Therefore, only the steep slopes provide a favorable environment for small-scale gravitational slumping that can be triggered by strong shaking during big seismic events.

6.3.1. San Pedro Escarpment

The San Pedro escarpment shows a clear surface expression probably related to its origin with the activity of HFZ (HFZ in Figure 6). Assuming this interpretation, the HFZ is a large fault with no recent activity (Pérez-Estaún et al., 2007), and the marine seismic sections only show gravitational deformation near the escarpment. In addition, there is no seismicity that could be associated with any activity in a deep-rooted fault of this scarp.

15252027, 2025, 6, Downloaded from https://agupubs.onlinelibrary.wiley.com/doi/10.1029/2024GC012092 by Universidad Complutense De, Wiley Online Library on [02/06/2025]. See the Terms and Conditions (https://onlinelibrary.wiley.com/terms-and-conditions) on Wiley Online Library for rules of use; OA articles are governed by the applicable Creative Commons License

However, because of the steep slope, it is prone to submarine landslides with tsunami potential because of strong coseismic shaking or sediment slope accumulation.

6.3.2. Saona Ridge

The Saona ridge has a significant seafloor expression, but there is no evidence of recent tectonic activity on faults rooting the structure (Figure 11). Most of the seismic events on the Saona ridge have a focal depth beneath the basal detachment of the MTB and are related to flexural slip processes in the CARIB LIP slab (Events 4, 5 and 6 in Figure 4). The focal mechanism 1 is shallower located along the detachment, showing a pure reverse solution. This mechanism is much more coherent with a rupture along the MFT or MMS because a potential rupture along the Saona ridge should show a normal or strike-slip component (Gorosabel-Araus et al., 2021; Granja-Bruña et al., 2014). The slopes flanking the Saona ridge are characterized using small scale gravitational processes. Some of the head scarps in the south slope show irregular morphology, suggesting the sequential occurrence of small slumps and then having low potential of tsunami. The two bigger slumps have an extension of 66 km2 but the average thickness is only 100 m, resulting in a volume of ≈6.6 km^3 with limited tsunami potential (Yellow stars in Figure 6).

6.3.3. Punta Palenque High

In the upper slope region, most of the imbricate structure of the MTB is buried beneath the sediments of the SPB. The overall imbricate structure seems to have low tectonic activity, but one of these thrusts forms a fault-propagation fold that deforms the seafloor, but the fault does not reach the surface (Muertos Rear Thrust, MRT in Figures 6, 12 and 15). The anticline ridge observed in the seafloor for 35 km along the strike seems to be a recent feature because of its well-preserved morphology. The MRT could be aseismic, but it could also be connected in depth with the mega-splay faults or indeed the basal detachment. The orientation of the thrust fits well with the orientation of the nodal planes of the focal mechanism of the Muertos Shallow Group (Figures 4 and 5). Also, the steeper nodal plane fits well with the sub-vertical geometry of the thrust. Assuming a worse-case scenario with a complete rupture of 35 km of length and 6 km of width, and a pure reverse motion, this rupture area can generate a Mw 6.4 event (Figure 15, Table 1. Figure S3g in Supporting Information S1).

The Punta Palenque faults are affected by extensional deformation characterized by a dense normal fault system (Figure 6). Most faults are shallow-rooted faults, but some of them could evolve into gravity instabilities, yielding tsunami potential. Some of the bigger faults can be observed by 40 km in length; however, they are surficial ruptures and do not reach the seismogenic depth. Their threat is because gravity failures can be nucleated along these faults and a slump can be triggered during strong shaking.

6.4. Beata Ridge Fault Zone (BRFZ)

The eastern and western flanks of Beata ridge do not show recent tectonic deformation. They are dominated using diffuse gravity-driven slope processes (canyons and small slumping). The only zone with active deformation is located along the summit showing a NW-SE oriented zone of extension probably controlled by gravitational and isostatic processes (BRFZ in Figure 15; Granja-Bruña et al., 2014). This fault zone shows many fault segments arranged in an echelon. These faults seem to be superficial and aseismic as it is attested by the absence of significant seismicity. Assuming a worse-case scenario with a complex rupture including several connected small segment faults (i.e., rupture area: 90 km of length x 6 km of width), it could yield events of Mw6.1. Considering a more likely scenario with a rupture length of 20 km, it could yield moderate magnitude earthquakes (Mw4.5–5.5) with a limited tsunamigenic potential (BRFZ in Table 1, Figure S3g in Supporting Information S1). However, the strong shaking of large events nucleated in the MTB and/or onshore in the Beata indentation area have the potential to trigger submarine landslides in the steep seafloor of the Beata ridge having tsunamigenic potential. Gravity instabilities in the steep island slope of the Southern Peninsula of Haiti were suggested as the tsunami source related to the strong shaking during the 2010 Mw7.0 Haiti event (Poupardin et al., 2020).

7. Summary and Conclusions

Historical and instrumental data suggest that the southern insular margin of the Dominican Republic is prone to large earthquakes and potential tsunamis. Because of the proximity of seismic and tsunami sources, this region

15252027, 2025, 6, Downloaded from https://agupubs.onlinelibrary.wiley.com/doi/10.1029/2024GC012092 by Universidad Complutense De, Wiley Online Library on [02/06/2025]. See the Terms and Conditions (https://onlinelibrary.wiley.com/terms-and-conditions) on Wiley Online Library for rules of use; OA articles are governed by the applicable Creative Commons License

can be seen as being at a clear risk. The combined interpretation of seismotectonic, offshore seismic reflection and multibeam bathymetry allowed us to identify the active processes and characterize the most significant near-field tectonic and landslide tsunami sources. By employing semi-empirical relationships based on location, size, geometry, and rupture mechanism data from tectonic sources, it is possible to estimate the potential magnitude of future seismic events.

The seismotectonic analysis based on the spatial distribution of seismicity with Mw > 4.5 and the focal mechanisms suggest the existence of three earthquake groups that can be related to the two main tectonic processes taking place in the southern Hispaniola: the underthrusting the interior of the CARIB plate (CARIB LIP) beneath the island arc along the Muertos margin and the collision-indenting of the Beata ridge against island arc in the south-central Hispaniola. The underthrusting of the CARIB LIP shows a shallow earthquake group related to compressive deformation in the Muertos thrust belt and a deeper group associated with flexural intra-slab events. The shallow group shows dominant reverse focal mechanisms that are associated with large ruptures along the basal detachment and the thrust faults in the Muertos thrust belt that could deform and rupture the seafloor, possibly causing a tsunami. The focal depths of the deep group are too big to cause seafloor deformation/rupture, but because of the strong shaking, they could trigger submarine landslides causing tsunamis. The indenting of the Beata ridge yields focal mechanisms varying in type in agreement with the indenter morphology. Those events are located onshore, but because of the shallow focal depths, the strong shaking, and the proximity of the seismic sources to the steep offshore areas, they could trigger submarine landslides causing tsunamis.

The Muertos margin province shows widespread active tectonic and sedimentary processes, whereas the Venezuelan basin and the Beata ridge provinces only show local zones of active processes. The major tectonic sources of tsunami are in the Muertos margin and entail large megathrust shallow faults that can generate significant magnitude seismic events with enough energy released to deform and occasionally rupture the seafloor and consequently generate a significant tsunami: Muertos frontal thrust (MFT), Muertos mega-splay (MMS), Muertos trough fault zone (MTFZ). All sources are dip-slip reverse and normal faults having the capacity to deform the seafloor vertically augmenting the tsunami potential. The Muertos margin could yield big events like subduction-earthquakes with significant magnitudes, as documented in the instrumental records (Mw6.7 in 1984). The historical records, although not conclusive, suggest that the event occurred the 18th of October of 1751 could be associated with the Muertos margin, where there are capable faults to nucleate large events such as the MFT and MMS. MFT and MMS, because of their large size, geometry, seafloor expression and seismotectonic characteristics related to the Muertos shallow group, must be considered as major direct and indirect potential sources of tsunami.

The worst-case scenarios for tsunami in the study area caused by tectonic sources would be large ruptures along the MTFZ, MFT or MMS. These tectonic sources have the capacity to generate events of magnitude 7 and bigger and have enough energy release to significantly deform the seafloor causing tsunamis.

The steeper seafloor slopes of the study area show frequent evidence of active gravitational processes. Most of the gravity failures are concentrated in the upper and middle slopes of the Muertos margin because of over-steepening of the tapered seafloor slope. The gravity instabilities have a relatively limited size, with widespread minor slumping and head scarps controlled using sequential processes, and initially have small tsunamigenic potential. Only the large Complutense slump was identified as a worst-case scenario of landslides with a high potential of tsunami. This slump has mobilized ≈30 km^3 of material and is located along the surface trace of the large active Muertos mega-splay fault. The continuous head scarp suggests a single event, but the absence of slump deposits indicates this event is not recent. If a similar volume is mobilized in a single and quick slide, it could generate a significant tsunami.

The Dominican Republic government must consider tsunami simulations for practical implementation of tsunami preparedness and protection for coastal planning and marine resource use. The southern coast is at obvious risk because of the proximity of the potential tsunamigenic sources to the coastal areas (30–50 km), resulting in a very short lead-time for response (less than 10 min). Although the southern coast is often characterized by terraced morphology and cliffs providing natural protection from tsunamis, there are many local vulnerable zones, such as beaches, river mouths, bays, and ports, where the tsunami wave is amplified, causing significant damage.

Data Availability Statement

Seismological data used in the study are public via the National Earthquake Information Center (NEIC-USGS) and the CMT Catalog (Ekström et al., 2012) accessed in March of 2023. Marine data used in the study were published in the literature (Andrews et al., 2014; Granja-Bruña et al., 2014) and in the Supporting Information S1 and S2.

Acknowledgments
This work was supported by the Spanish Agency of Research (Caribbean Projects: REN2003-08520; CTM2006-13666, CGL2010-17715, and PID2022-138360NB-I00) and by the U.S. Geological Survey Coastal and Marine Geology Program (Caribbean earthquake and tsunami hazards project). We are indebted to the crew and technicians of the R/V Hespérides, Sarmiento de Gamboa and Ron Brown for their professional help at sea. The professional work of the technicians of the Unidad de Tecnología Marina is greatly appreciated. This work was also partially funded by CARESOIL (S2013/MAE-2739), I+D CARESOIL (S2018/EMT-4317) and MARIBNO projects (PGC2018-095999-B-I00). Some figures were drafted using the free software Generic Mapping Tools v5.0 (Wessel et al., 2013). We would like to thank the anonymous reviewers for their valuable revision and suggestions to improve the quality of the paper.

References

Ali, S. T., Freed, A. M., Calais, E., Manaker, D. M., & McCann, W. (2008). Coulomb stress evolution in Northeastern Caribbean over the past 250 years due to coseismic, postseismic and interseismic deformation. *Geophysical Journal International*, *174*(3), 904–918. https://doi.org/10.1111/j.1365-246x.2008.03634.x

Álvarez-Gómez, J. A. (2019). FMC—Earthquake focal mechanisms data management, cluster and classification. *SoftwareX*, *9*, 299–307. https://doi.org/10.1016/j.softx.2019.03.008

Andrews, B. D., ten Brink, U., Danforth, W. W., Chaytor, J. D., Granja-Bruña, J. L., Llanes, P., & Carbó-Gorosabel, A. (2014). *Bathymetric terrain model of Puerto Rico Trench and the Northeast Caribbean Region for marine geological investigations*. U.S. Geological Survey Open-File Report 2013–1125. Retrieved from http://pubs.usgs.gov/of/2013/1125/

Ayala, C., García-Lobón, J. L., Escuder-Viruete, J., Rey Moral, C., Pérez-Estaún, A., & Padín-Debén, A. (2017). High resolution magnetic, regional gravity and petrophysical characterization of the Dominican Republic tectonic domains with special focus on the Central Cordillera. *Boletin Geologico y Minero*, *128*(3), 611–631. https://doi.org/10.21701/bolgeomin.128.3.005

Bakun, W. H., Flores, C. H., & ten Brink, U. (2012). Significant earthquakes on the Enriquillo Fault system, Hispaniola, 1500-2010: Implications for seismic hazard. *Bulletin of the Seismological Society of America*, *102*(No.1), 18–30. https://doi.org/10.1785/0120110077

Bangs, N. L. B., Moore, G. F., Gulick, S. P. S., Pangborn, E. M., Tobin, H. J., Kuramoto, S., & Taira, A. (2009). Broad, weak regions of the Nankai Megathrust and implications for shallow coseismic slip. *Earth and Planetary Science Letters*, *284*(1–2), 44–49. https://doi.org/10.1016/j.epsl.2009.04.026

Beckers, J., & Lay, T. (1995). Very broadband seismic analysis of the 1992 Flores, Indonesia, earthquake (Mw = 7.9). *Journal of Geophysical Research*, *100*(B9), 18179–18193. https://doi.org/10.1029/95JB01689

Byrne, D. B., Suárez, G., & McCann, W. R. (1985). Muertos trough subduction, microplate tectonics in the northern Caribbean? *Nature*, *317*(6036), 420–421. https://doi.org/10.1038/317420a0

Calais, E., Freed, A., Mattioli, G., Amelung, F., Jónsson, S., Jansma, P., et al. (2010). Transpressional rupture of an unmapped fault during the 2010 Haiti earthquake. *Nature Geoscience*, *3*(11), 794–799. https://doi.org/10.1038/ngeo992

Calais, E., Mazabraud, Y., Mercier de Lepinay, B., Mann, P., Mattioli, G., & Jansma, P. (2002). Strain partitioning and fault slip rates in the northeastern Caribbean from GPS measurements. *Geophysical Research Letters*, *29*(18), 1856. https://doi.org/10.1029/2002GL015397

Calais, E., Symithe, S., Mercier de Lépinay, B., & Prépetit, C. (2016). Plate boundary segmentation in the northeastern Caribbean from geodetic measurements and Neogene geological observations. *C. R. Geoscience*, *348*, 42–51. https://doi.org/10.1016/j.crte.2015.10.007

Calais, E., Symithe, S. J., & Mercier de Lépinay, B. (2022). Strain partitioning within the Caribbean–North America transform plate boundary in Southern Haiti, tectonic and hazard implications. *Bulletin of the Seismological Society of America*, *113*, 131–142. https://doi.org/10.1785/0120220121

Chacón-Barrantes, S., & Zamora, N. (2017). Numerical simulations of the 1991 Limón tsunami, Costa Rica Caribbean coast. *Pure and Applied Geophysics*, *174*(8), 2945–2959. https://doi.org/10.1007/s00024-017-1631-x

DeMets, C., Gordon, R. G., & Argus, D. F. (2010). Geologically current plate motions. *Geophysical Journal International*, *181*, 1–80. https://doi.org/10.1111/j.1365-246X.2009.04491.x

Didenkulova, I., Romano, F., Armigliato, A., Hebert, H., Murphy, S., Sallares, V., et al. (2021). Tsunamis: From source processes to coastal hazard and warning. *Natural Hazards and Earth System Sciences*.

Dillon, W. P., Edgar, N. T., Scanlon, K. M., & Coleman, D. F. (1996). A review of the tectonic problems or the strike-slip northern Boundary of the Caribbean plate and examination by GLORIA. In J. V. Gardner, M. E. Field, & D. C. Twichel (Eds.), *Geology of the United States Seafloor: The view from GLORIA* (Vol. 9, pp. 135–164). Cambridge University Press.

Dolan, J. F., Mullins, H. T., & Wald, D. J. (1998). Active tectonics of the north-central Caribbean; oblique collision, strain partitioning, and opposing subducted slabs. In *Active Strike-slip and Collisional Tectonics of the Northern Caribbean Plate Boundary Zone*. (ISBN: 0813723264).

Driscoll, N. W., & Diebold, J. B. (1999). Tectonic and stratigraphic development of the eastern Caribbean: New constraints from multichannel seismic data In K. J. Hsü, & P. Mann, (Eds.). *Sedimentary Basins of the World, 4. Caribbean Basins* (pp. 591–626). Elsevier Science.

Dunán-Avila, P., Authemayou, C., Jaud, M., Pedoja, K., Jara-Muñoz, J., Bertin, S., et al. (2025). Geomorphological signatures of known hurricanes and validation of theoretical emplacement formulations: Coastal boulder deposits on Cuban low-lying marine terraces. *Marine Geology*, *480*, 107438. https://doi.org/10.1016/j.margeo.2024.107438

Ekström, G., Nettles, M., & Dziewonski, A. M. (2012). The global CMT project 2004-2010: Centroid-moment tensors for 13,017 earthquakes. *Physics of the Earth and Planetary Interiors*, *200–201*, 1–9. https://doi.org/10.1016/j.pepi.2012.04.002

Engel, M., Oetjen, J., May, S. M., & Brückner, H. (2016). Tsunami deposits of the Caribbean—Towards an improved coastal hazard assessment. *Earth-Science Reviews*, *163*(2016), 260–296. https://doi.org/10.1016/j.earscirev.2016.10.010

Escuder-Viruete, J., Fernández, F. J., Pérez Valera, F., & McDermott, F. (2024). Active tectonics, Quaternary stress regime evolution and seismotectonic faults in southern central Hispaniola: Implications for the quantitative seismic hazard assessment. *Geochemistry, Geophysics, Geosystems*, *25*(2), e2023GC011003. https://doi.org/10.1029/2023GC011003

Escuder-Viruete, J., Fernández, F. J., Pérez Valera, F., & Medialdea, A. (2023). Present-day accommodation of Caribbean-North American oblique plate convergence through the Ocoa-Bonao-La Guacara fault zone, southern central Hispaniola: A transition zone between oceanic subduction and arc-oceanic plateau collision. *Tectonics*, *42*(4), e2022TC007618. https://doi.org/10.1029/2022TC007618

Farr, T. G., Rosen, P. A., Caro, E., Crippen, R., Duren, R., Hensley, S., et al. (2007). The shuttle radar topography mission. *Reviews of Geophysics*, *45*(2). https://doi.org/10.1029/2005RG000183

Felix, R. P., Hubbard, J. A., Bradley, K. E., Lythgoe, K. H., Li, L., & Switzer, A. D. (2022). Tsunami hazard in Lombok and Bali, Indonesia, due to the Flores back-arc thrust. *Natural Hazards and Earth System Sciences*, *22*(5), 1665–1682. https://doi.org/10.5194/nhess-22-1665-2022

15252027, 2025, 6, Downloaded from https://agupubs.onlinelibrary.wiley.com/doi/10.1029/2024GC012092 by Universidad Complutense De, Wiley Online Library on [02/06/2025]. See the Terms and Conditions (https://onlinelibrary.wiley.com/terms-and-conditions) on Wiley Online Library for rules of use; OA articles are governed by the applicable Creative Commons License

Flores, C. H., ten Brink, U. S., & Bakun, W. H. (2012). Accounts of damage from historical earthquakes in the northeastern Caribbean to aid in the determination of their location and intensity magnitudes. Open-File Report 2011-1133. https://doi.org/10.3133/ofr20111133

Fritz, H. M., Vilmond Hillaire, J., Molière, E., Wei, Y., & Mohammed, F. (2012). Twin tsunamis triggered by the 12 January 2010 Haiti earthquake. *Pure and Applied Geophysics*, *170*(9–10), 1463–1474. https://doi.org/10.1007/s00024-012-0479-3

Frohlich, C. (1992). Triangle diagrams: Ternary graphs to display similarity and diversity of earthquake focal mechanisms. *Physics of the Earth and Planetary Interiors*, *75*(1–3), 193–198. https://doi.org/10.1016/0031-9201(92)90130-n

García-Senz, J., Escuder-Viruete, J., & Pérez-Estaún, A. (2017). Geometría, cinemática, paleoesfuerzos y modelo tectónico del sistema de fallas extensionales que deforma a las calizas Plio-Pleistocenas en el sureste de la República Dominicana. *Boletin Geologico y Minero*, *128*(3), 695–714. https://doi.org/10.21701/bolgeomin.128.3.009

Geist, E., Fritz, H. M., Rabinovich, A. B., & Tanioka, Y. (2016). Introduction to "global tsunami science": Past and future, volume I. *Pure and Applied Geophysics*, *173*(2016), 3663–3669. https://doi.org/10.1007/s00024-016-1427-4

Gorosabel-Araus, J. M., Granja-Bruña, J. L., Gallego-Mingo, A., Gómez de la Peña, L., Rodríguez-Zurrunero, A., Mas, R., et al. (2021). New constraints on the tectono-sedimentary evolution of the offshore San Pedro Basin (South-Eastern Dominican Republic): Implications for its hydrocarbon potential. In I. Davidson, J. N. F. Hull, & J. Pindell (Eds.), *The Basins, Orogens and Evolution of the Southern Gulf of Mexico and Northern Caribbean* (Vol. 504, pp. 479–505). Geological Society of London, Special Publications. https://doi.org/10.1144/SP504-2019-224

Granja-Bruña, J. L., Carbó-Gorosabel, A., Llanes, P., Muñoz-Martín, A., ten Brink, U. S., Gómez Ballesteros, M., et al. (2014). Morphostructure at the junction between the Beata ridge and the Greater Antilles island arc (offshore Hispaniola southern slope). *Tectonophysics*, *618*, 138–163. https://doi.org/10.1016/j.tecto.2014.02.001

Granja-Bruña, J. L., Muñoz-Martín, A., ten Brink, U. S., Carbó-Gorosabel, A., Llanes, P., Córdoba-Barba, D., et al. (2010). Gravity modeling of the Muertos Trough and tectonic implications (NE Caribbean). *Marine Geophysical Researches*, *31*(4), 263–283. https://doi.org/10.1007/s11001-010-9107-8

Granja-Bruña, J. L., ten Brink, U. S., Carbó-Gorosabel, A., Muñoz-Martín, A., & Gómez Ballesteros, M. (2009). Morphotectonics of the central Muertos thrust belt and Muertos Trough (northeastern Caribbean). *Marine Geology*, *263*(1–4), 7–33. https://doi.org/10.1016/j.margeo.2009.03.010

Granja-Bruña, J. L., ten Brink, U. S., Muñoz-Martín, A., Llanes, P., & Carbó-Gorosabel, A. (2015). Tectonic geomorphology of the southern Puerto Rico offshore margin. *Marine and Petroleum Geology*, *67*, 30–56. https://doi.org/10.1016/j.marpetgeo.2015.04.014

Grindlay, N. R., Hearne, M., & Mann, P. (2005). High risk of tsunami in the northern Caribbean. *EOS American Geophysical Union*, *86*(12), 121–126. https://doi.org/10.1029/2005EO120001

Hallo, M., Opršal, I., Asano, K., & Gallovic, F. (2019). Seismotectonics of the 2018 northern Osaka M6.1 earthquake and its aftershocks: Joint movements on strike-slip and reverse faults in inland Japan. *Earth Planets and Space*, *71*(1), 34. https://doi.org/10.1186/s40623-019-1016-8

Harbitz, C. B., Glimsdal, S., Bazin, S., Zamora, N., Løvholt, F., Bungum, H., et al. (2012). Tsunami hazard in the Caribbean: Regional exposure derived from credible worst-case scenarios. *Continental Shelf Research*, *8*, 1–23. https://doi.org/10.1016/j.csr.2012.02.006

Hernáiz-Huerta, P. P., Diaz de Neira, J. A., García-Senz, J., Deschamps, I., Genna, A., Nicole, N., et al. (2007). La estructura del suroeste de la República Dominicana: un ejemplo de deformación en régimen transpresivo. *Boletin Geologico y Minero*, *118*(2), 337–357.

Heubeck, C., & Mann, P. (1991). Structural geology and Cenozoic tectonic history of the southeastern termination of the Cordillera Central, Dominican Republic. *Geological Society of America Special Paper*, *262*, 315–336. https://doi.org/10.1130/spe262-p315

Iida, K. (1970). The generation of tsunamis and the focal mechanism of earthquakes. In W. M. Adams (Ed.), *Tsunamis in the Pacific Ocean* (pp. 3–18). East-West Center Press.

IOC Workshop report No 276. (2016). *Sources of tsunamis in the Caribbean with possibility to impact the southern coast of the Dominican Republic, Santo Domingo*. Intergovernmental Oceanographic Commission UNESCO (pp. 36. IOC/2016/WR/276 Rev.).

Jansma, P. E., & Mattioli, G. S. (2005). GPS results from Puerto Rico and the Virgin Islands: Constraints on tectonic setting and rates of active faulting. In P. Mann (Ed.), *Active Tectonics and Seismic Hazards of Puerto Rico, the Virgin Islands, and Offshore Areas* (p. 13e30). Geological Society of America. Special Paper 385.

Kumar, S., Agrawal, M., & Pulliam, J. (2023). Modeling seismic anisotropy beneath the Island of Hispaniola via the harmonic decomposition of receiver functions. *Geochemistry, Geophysics, Geosystems*, *24*(5), e2022GC010773. https://doi.org/10.1029/2022GC010773

Kumar, S., Agrawal, M., Pulliam, J., Polanco Rivera, E., & Huerfano, V. (2020). Crustal thickness and bulk Poisson ratios in the Dominican Republic from receiver function analysis. *Tectonophysics*, *775*, 228308. https://doi.org/10.1016/j.tecto.2019.228308

Lagabrielle, Y., Pelletier, B., Cabioch, G., Regnier, M., & Calmant, S. (2003). Coseismic and long-term vertical displacement due to back arc shortening, central Vanuatu; offshore and onshore data following the Mw 7.5, 26 November 1999 Ambrym earthquake. *Journal of Geophysical Research*, *108*(B11), 5. https://doi.org/10.1029/2002JB002083

Llanes, P., ten Brink, U., Granja-Bruña, J. L., Carbó-Gorosabel, A., Flores, C., Villaseñor, A., et al. (2012). True subduction vs. underthrusting of the Caribbean plate beneath Hispaniola, northern Caribbean. In *American Geophysical Union Fall Meeting EOS, Fall Meet. Suppl., Abstract T13A-2567*.

López-Venegas, A. M., Chacón, S., Zamora, N., Audemard, F., Dondin, F., Clouard, V., et al. (2015). Tsunamis from tectonic sources along Caribbean plate boundaries, poster. In *AGU Fall Meeting, December 2015*.

López-Venegas, A. M., Horrillo, J., Pampell-Manis, A., Huérfano, V., & Mercado, A. (2014). Advanced tsunami numerical simulations and energy considerations by use of 3D–2D coupled models: The October 11, 1918, Mona passage tsunami. *Pure and Applied Geophysics*. https://doi.org/10.1007/s00024-014-0988-3

López-Venegas, A. M., ten Brink, U. S., & Geist, E. L. (2008). Submarine landslide as the source for the October 11, 1918 Mona passage tsunami: Observations and modeling. *Marine Geology*, *254*(1–2), 35–46. https://doi.org/10.1016/j.margeo.2008.05.001

Ludwig, R. (1989). *Double subduction beneath Hispaniola? An investigation of earthquakes by body wave inversion. MSc thesis* (p. 88). Oregon State University.

Manaker, D., Calais, E., Freed, A., Ali, T., Przybylski, P., Mattioli, G. S., et al. (2008). Interseismic plate coupling and strain partitioning in the Northeastern Caribbean. *Geophysical Journal International*, *174*(3), 889–903. https://doi.org/10.1111/j.1365-246x.2008.03819.x

Mann, P., Calais, E., Ruegg, J. C., DeMets, C., & Jansma, P. E. (2002). Oblique collision in the North-Eastern Caribbean from GPS measurements and geological observations. *Tectonics*, *2*(6), 1057. https://doi.org/10.1029/2001TC0011304

Mann, P., Taylor, F. W., Edwards, R. L., & Ku, T. L. (1995). Actively evolving microplate formation by oblique collision and sideways motion along strike–slip faults: An example from North-Western Caribbean plate margin. *Tectonophysics*, *246*(1–3), 1–69. https://doi.org/10.1016/0040-1951(94)00268-e

Mauffret, A., & Leroy, S. (1999). Neogene intraplate deformation of the Caribbean plate at the Beata Ridge. In K. J. Hsü, & P. Mann, (Eds.). *Sedimentary Basins of the World, 4. Caribbean Basins* (pp. 627–669). Elsevier Science.

15252027, 2025, 6, Downloaded from https://agupubs.onlinelibrary.wiley.com/doi/10.1029/2024GC012092 by Universidad Complutense De, Wiley Online Library on [02/06/2025]. See the Terms and Conditions (https://onlinelibrary.wiley.com/terms-and-conditions) on Wiley Online Library for rules of use; OA articles are governed by the applicable Creative Commons License

Mauffret, A., Leroy, S., Vila, J.-M., Hallot, E., de Lepinay, B. M., & Duncan, R. A. (2001). Prolonged magmatic and tectonic development of the caribbean igneous province revealed by a diving submersible survey. *Marine Geophysical Researches*, *22*, 17–45.

McCann, W. R. (2006). Estimating the threat of tsunamogenic earthquakes and earthquake induced landslide tsunami in the Caribbean. In A. Mercado & P. Liu (Eds.), *Caribbean Tsunami Hazard* (pp. 43–65). World Scientific Publishing.

McCann, W. R., & Sykes, L. R. (1984). Subduction of aseismic ridges beneath the Caribbean plate: Implications for the tectonics and seismic potential of the northeastern Caribbean. *Journal of Geophysical Research*, *89*(B6), 4493–4519. https://doi.org/10.1029/jb089ib06p04493

Moore, G. F., Bangs, N. L., Taira, A., Kuramoto, S., Pangborn, E., & Tobin, H. J. (2007). Three-dimensional splay fault geometry and implications for tsunami generation. *Science*, *318*(5853), 1128–1131. https://doi.org/10.1126/science.1147195

Moreau de Saint Méry, M. (1796). Description Topographique et Politique de la Partie Espagnole de L´isle Saint-Domingue. In S. D. Bibliófilos (Ed.), *Filadelfia, USA: Editora de Santo Domingo, 1976* (Vol. I).

NCEI database. (n.d.). *National centers for environmental information*. National Oceanic and Atmospheric Administration. Retrieved from https://www.ncei.noaa.gov/products/natural-hazards/tsunamis-earthquakes-volcanoes/tsunamis

NEIC-USGS. (n.d.). *National earthquake information center*. U.S. Geological Survey. Retrieved from https://www.usgs.gov/programs/earthquake-hazards/earthquakes

Noda, A. (2016). Forearc basins: Types, geometries, and relationships to subduction zone dynamics. *Geological Society of America Bulletin*, *128*(5–6), 879–895. https://doi.org/10.1130/B31345.1

Nuñez, D., Córdoba, D., Cotilla, M. O., & Pazos, A. (2016). Modelling the crust and upper mantle in northern Beata Ridge (CARIBE NORTE project). *Pure and Applied Geophysics*, *173*(5), 1639–1661. https://doi.org/10.1016/j.tecto.2019.228224

Núñez, D., Córdoba, D., & Kissling, E. (2019). Seismic structure of the crust in the western Dominican Republic. *Tectonophysics*, *773*, 228224. https://doi.org/10.1016/j.tecto.2019.228224

Okal, E. (2017). The excitation of tsunamis by deep earthquakes. *Geophysical Journal International*, *209*, 234–249.

Oliveira de Sá, A., Leroy, S., d'Acremont, E., Lafuerza, S., Granja-Bruña, J. L., Momplaisir, R., et al. (2025). Analysis of seismic reflection data from the Northern Hispaniola margin: Implications for the recent evolution of the Northern Caribbean Plate boundary. *Tectonophysics*, *904*(2025), 230714. https://doi.org/10.1016/j.tecto.2025.230714

O'Loughlin, K. F., & Lander, J. F. (2003). *Caribbean tsunamis: A 500-year history from 1498-1998*. Kluwer Academic Publishers. (In cooperation with the National Oceanic and Atmospheric Administration [NOAA] and Cooperative Institute for Research in Environmental Sciences [CIRES], University of Colorado).

Pérez-Estaún, A., Hernaiz Huerta, P. P., Lopera, E., Joubert, M., Escuder-Viruete, J., Díaz de Neira, A., et al. (2007). Geología de la República Dominicana: De la construcción de arco-isla a la colisión arco-continente. *Boletin Geologico y Minero*, *118*, 157–174.

Possee, D., Rychert, C., Harmon, N., & Keir, D. (2021). Seismic discontinuities across the North American Caribbean plate boundary from S-to-P receiver functions. *Geochemistry, Geophysics, Geosystems*, *22*(7), e2021GC009723. https://doi.org/10.1029/2021GC009723

Poupardin, A., Calais, E., Heinrich, P., Hébert, H., Rodriguez, M., Leroy, S., et al. (2020). Deep submarine landslide contribution to the 2010 Haiti earthquake tsunami. *Natural Hazards and Earth System Sciences*, *20*(7), 2055–2065. https://doi.org/10.5194/nhess-20-2055-2020

Raimbault, B., Jolivet, R., Calais, E., Symithe, S., Fukushima, Y., & Dubernet, P. (2023). Rupture geometry and slipdistribution of the Mw 7.2 Nippes earthquake, Haiti, from space geodetic data. *Geochemistry, Geophysics, Geosystems*, *24*(4), e2022GC010752. https://doi.org/10.1029/2022GC010752

Reiter, F., Freudenthaler, C., Hausmann, H., Ortner, H., Lenhardt, W., & Brandner, R. (2018). Active seismotectonic deformation in front of the Dolomites indenter, Eastern Alps. *Tectonics*, *37*(12), 4625–4654. https://doi.org/10.1029/2017TC004867

Rodríguez, J. (2019). Terremoto del 18 de octubre del 1751. *Geonoticias*, *16*(45), 38–41.

Rodríguez, J., Havskov, J., Sorensen, M., & Santos, L. (2018). Seismotectonics of south-west Dominican Republic. *Journal of Seismology*, *22*(4), 883–896. https://doi.org/10.1007/s10950-018-9738-9

Rodríguez-Zurrunero, A., Granja-Bruña, J. L., Carbó-Gorosabel, A., Muñoz-Martín, A., Gorosabel-Araus, J. M., Gómez de la Peña, L., et al. (2018). Submarine morpho-structure and active processes along the North American-Caribbean plate boundary (Dominican Republic sector). *Marine Geology*, *407*, 121–147. https://doi.org/10.1016/j.margeo.2018.10.010

Rodríguez-Zurrunero, A., Granja-Bruña, J. L., Muñoz-Martín, A., Leroy, S., ten Brink, U., Gorosabel-Araus, J. M., et al. (2020). Along-strike segmentation in the northern Caribbean plate boundary zone (Hispaniola sector): Tectonic implications. *Tectonophysics*, *618*, 138–163. ISSN: 0040-1951. https://doi.org/10.1016/j.tecto.2014.02.001

Romeo, I., & Álvarez-Gómez, J. A. (2018). Lithospheric folding by flexural slip in subduction zones as source for reverse fault intraslab earthquakes. *Scientific Reports*, *8*(1), 1367. https://doi.org/10.1038/s41598-018-19682-7

Scardino, G., Rovere, A., Barile, C., Nandasena, N. A. K., Chauveau, D., Dahm, M., et al. (2025). Coastal boulders emplaced by extreme wave events impacting the ABC islands (Aruba, Bonaire, Curaçao; Leeward Antilles, Caribbean). *Quaternary Science Reviews*, *349*, 109136. https://doi.org/10.1016/j.quascirev.2024.109136

Scherer, J. (1912). Great earthquakes in the island of Haiti. *Bulletin of the Seismological Society of America*, *2*(3), 161–180. https://doi.org/10.1785/bssa0020030161

Stern, R. J., & Gerya, T. (2018). Subduction initiation in nature and models: A review. *Tectonophysics*, *746*, 173–198. https://doi.org/10.1016/j.tecto.2017.10.014

Suárez, G., Pardo, M., Dominguez, J., Ponc, L., Montero, W., Boschini, I., & Rojas, W. (1995). The Limon, Costa Rica earthquake of April 22, 1991; back arc thrusting and collisional tectonics in a subduction environment. *Tectonics*, *14*, 518–530. https://doi.org/10.1029/94TC02546

ten Brink, U. S., Bakun, W. H., & Flores, C. H. (2011). Historical perspective on seismic hazard to Hispaniola and the northeast Caribbean region. *Journal of Geophysical Research*, *106*(Issue B12).

ten Brink, U. S., Bakun, W. H., & Flores, C. H. (2013). Seismic hazard from the Hispaniola subduction zone: Correction to "Historical perspective on seismic hazard to Hispaniola and the northeast Caribbean region". *Journal of Geophysical Research: Solid Earth*, *118*(10), 5597–5600. https://doi.org/10.1002/jgrb.50388

ten Brink, U. S., & López-Venegas, A. (2012). Plate interaction in the NE Caribbean subduction zone from continuous GPS observations. *Geophysical Research Letters*, *39*(10), L10304. https://doi.org/10.1029/2012GL051485

ten Brink, U. S., Marshak, S., & Granja-Bruña, J. L. (2009). Bivergent thrust wedges surrounding oceanic island arcs: Insight from observations and sandbox models of the northeastern Caribbean plate. *Geological Society of America Bulletin*, *121*(11–12), 1522–1536. https://doi.org/10.1130/B26512.1

ten Brink, U. S., Wei, Y., Fan, W., Granja-Bruña, J. L., & Miller, N. (2020). Mysterious tsunami in the Caribbean Sea following the 2010 Haiti earthquake possibly generated by dynamically triggered early aftershocks. *Earth and Planetary Science Letters*, *540*(15 June 2020), 116269. https://doi.org/10.1016/j.epsl.2020.116269

15252027, 2025, 6, Downloaded from https://agupubs.onlinelibrary.wiley.com/doi/10.1029/2024GC012092 by Universidad Complutense De, Wiley Online Library on [02/06/2025]. See the Terms and Conditions (https://onlinelibrary.wiley.com/terms-and-conditions) on Wiley Online Library for rules of use; OA articles are governed by the applicable Creative Commons License

Terrier-Sedan, M., & Bertil, D. (2021). Active fault characterization and seismotectonic zoning of the Hispaniola Island. *Journal of Seismology*, *25*(2), 499–520. https://doi.org/10.1007/s10950-021-09985-0

Van Benthem, S., Govers, R., & Wortel, R. (2014). What drives microplate motion and deformation in the northeastern Caribbean plate boundary region? *Tectonics*, *33*(5), 850–873. https://doi.org/10.1002/2013TC003402

Von Hillebrandt-Andrade, C. (2013). Minimizing Caribbean tsunami risk. *Science*, *80*. https://doi.org/10.1126/science.1238943

Wang, K., & Bilek, S. L. (2011). Do subducting seamounts generate or stop large earthquakes? *Geology*, *39*(9), 819–822. https://doi.org/10.1130/G31856.1

Weatherall, P., Marks, K. M., Jakobsson, M., Schmitt, T., Tani, S., Arndt, J. E., et al. (2015). A new digital bathymetric model of the world's oceans. Earth Sp. *Science*, *2*(8), 331–345. https://doi.org/10.1002/2015EA000107

Wells, D. L., & Coppersmith, J. C. (1994). New empirical relationships among magnitude, rupture length, rupture width, rupture area and surface displacement. *Bulletin of the Seismological Society of America*, *84*(4), 974–1002. https://doi.org/10.1785/bssa0840040974

Wessel, P., Smith, W. H. F., Scharroo, R., Luis, J., & Wobbe, F. (2013). Generic mapping Tools: Improved Version released. *EOS, Transactions American Geophysical Union*, *94*(45), 409–410. https://doi.org/10.1002/2013EO450001

Xu, X., Keller, G. R., & Gou, X. (2015). Dip variations of the North American and North Caribbean Plates dominate the tectonic activity of Puerto Rico–Virgin Islands and adjacent areas. *Geological Journal*, *51*(6), 901–914. https://doi.org/10.1002/gj.2708

Yang, H., Liu, Y., & Lin, J. (2012). Effects of subducted seamounts on megathrust earthquake nucleation and rupture propagation. *Geophysical Research Letters*, *39*(24), L24302. https://doi.org/10.1029/2012GL053892

Reference From the Supporting Information

Carbó-Gorosabel, A., Córdoba-Barba, D., Martín-Dávila, J., Granja-Bruña, J. L., Llanes, P., Muñoz-Martín, A., & ten Brink, U. S. (2010). Exploring active tectonics in the Dominican Republic. (Vol. *91*pp. 261–268). (27July2010).

15252027, 2025, 6, Downloaded from https://agupubs.onlinelibrary.wiley.com/doi/10.1029/2024GC012092 by Universidad Complutense De, Wiley Online Library on [02/06/2025]. See the Terms and Conditions (https://onlinelibrary.wiley.com/terms-and-conditions) on Wiley Online Library for rules of use; OA articles are governed by the applicable Creative Commons License